COURSE 11

SINGLE ELECTRON PHENOMENA IN METALLIC NANOSTRUCTURES

Michel H. Devoret, Daniel Esteve and Cristián Urbina

Groupe Quantronique
Service de Physique de l'Etat Condensé
CEA-Saclay, France

E. Akkermans, G. Montambaux, J.-L. Pichard and J. Zinn-Justin, eds.
Les Houches, Session LXI, 1994
Physique Quantique Mésoscopique
Mesoscopic Quantum Physics

Contents

1. Foreword

This course is divided into three parts. Its first part consists of a general discussion of single charge phenomena from a particular viewpoint: how to use these phenomena to transfer single charge quanta, i.e. electrons and Cooper pairs, one by one. This was the original goal of the teams that started to investigate single Cooper effects in the middle of the 80's. In this first part of the course, we will not use any mathematical formalism, but try to get the reader acquainted with the basic concepts and the orders of magnitude. The second part of the course is an introduction to the theory of non-superconducting mesoscopic tunnel junctions. The aim of this part is to explain the effect of the coupling of the junction, which can be thought of as a strong elastic electron scatterer, to its electromagnetic environment treated quantum mechanically. The quantum mechanical fluctuations of the charge resulting from this coupling are a crucial ingredient in our understanding of the dynamics of tunnel junction circuits. The third part of the course deals with superconducting circuits. One could naively think that single Cooper pairs in superconducting circuits take the role of single electrons in normal circuits. This will be possible only if there are no remaining unpaired electrons in the metallic electrodes of the circuit. We explain how the theory of superconductivity can be applied to a mesoscopic electrode to predict the conditions under which the transfer of a single Cooper pair is observable.

2. General overview of single charge phenomena

2.1. Introduction

One individual atom, a purely theoretical entity a hundred years ago, can now be imaged and manipulated at the surface of bulk matter [1] or, free-standing, in vacuum [2]. Is the electron, the simplest and most thoroughly studied particle, amenable to such ultimate control? In vacuum, the detection of single electrons is now routine. A spectacular example of the control of individual electrons travelling in a vacuum chamber is the experiment in which Dehmelt et al. [3] were able to probe during three months a single electron kept in an electromagnetic

trap, thereby measuring to unprecedented accuracy the anomalous part of its magnetic moment. In matter, the manipulation of individual electrons is a very different game, because the separation between electrons is of the same order as their quantum mechanical wavelength. Here we focus on the most basic type of such manipulation. We explain how it is possible to take, at a precise instant, exactly one electron from a first electrode and transfer it with certainty to a second electrode. By making these electrodes part of an electrical circuit and by continuously repeating this transfer process we can achieve a perfectly controlled current source. In particular, for a sequence of single-electron transfers clocked by a radiofrequency signal at frequency f, the current I will be given simply by $I = ef$ where e is the quantum of charge, a fundamental constant. We also qualitatively explain how, when at least one of the electrodes is in the superconducting state, electron pairing favors charge transfer by units of $2e$.

2.2. *Basic principles of single electron transfer*

Although the charge of the electron was measured as early as 1911 [4], the granularity of electricity does not usually show up in the macroscopic quantities such as current and voltage, which describe the state of an electric circuit. This is not just a matter of the number of electrons being very large in typical devices. Charge flow in a metal or a semiconductor is a continuous process because conduction electrons are not localized at specific positions. They form a quantum fluid which can be shifted by an arbitrary small amount. The variations of the charge Q on a capacitor C and of the associated potential difference $U = Q/C$ illustrate this property. The charge Q can be any fraction ε of the charge quantum e: if ρ denotes the electron density in the metallic plates of the capacitor and S their surface area, it is easy to see that a bodily displacement $\delta = \varepsilon/(\rho S)$ of the electronic fluid with respect to the ionic background, in the direction perpendicular to the plates, produces the charge $Q = \varepsilon e$.

There exists, however, a solid-state device in which electric charge flows in a discrete manner. It consists of two metallic electrodes separated by an insulating layer so thin that electrons can traverse it by quantum tunneling [5] (Fig. 1). Tunneling can be considered as an all-or-nothing process because electrons spend a negligible amount of time under the potential barrier corresponding to the insulating layer [6,7]. If one applies a voltage V to such a tunnel junction, electrons will randomly tunnel across the insulator at an average rate given by V/eR_t, where the tunnel resistance R_t is a macroscopic parameter of the junction which depends on the area and thickness of the insulating barrier. Apart from allowing the tunnel effect, the two facing electrodes behave as a capacitor whose capacitance C is the other macroscopic parameter of the junction. It is important to stress that the transport of electrons in a tunnel junction and in a metallic resistor are fun-

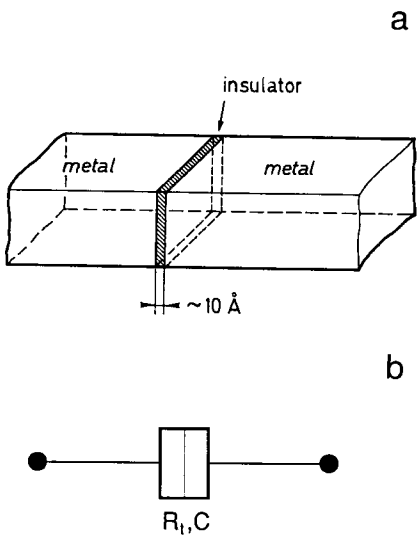

Fig. 1. a) A tunnel junction consists of two metallic electrodes separated by a thin insulating layer. When a fixed voltage is imposed to the junction, it is traversed by a current consisting of uncorrelated charge packets corresponding to individual electrons. Electrons tunnel through the thin layer of insulator which acts as a potential barrier. The junction is represented in circuit schematics by a double box symbol (b) and is characterized by the tunnel resistance R_t and capacitance C. It is worth noting that although R_t is called a "resistance", it characterizes a purely elastic process. At the insulating barrier, the electron wavefunction is partially transmitted and reflected. Its energy does not change. The tunnel resistance is inversely proportional to the barrier transmission coefficient which decreases exponentially with the thickness of the insulating layer. In practice, measurable tunnel resistances can be achieved only with insulating layers a few nanometres thick.

damentally different, even though the current–voltage characteristic is linear in both cases. Charge flows continuously along the resistor whereas it flows across the junction in packets of e. Obviously, a tunnel junction provides the means to extract electrons one at a time from an electrode. With a single voltage-biased tunnel junction, however, it is not possible to control the instants at which electrons pass from the upstream electrode to the downstream electrode, because of the stochastic nature of tunneling. A further ingredient is needed.

Suppose that instead of applying directly a voltage source to the junction one biases it with a voltage source U in series with a capacitor C_s (we reserve the letter symbol V for transport voltage sources that have to deliver a static current). A metallic electrode entirely surrounded by insulating material is formed between the junction and the capacitor (see Fig. 2a). We will call such an isolated electrode, which electrons can enter and leave only by tunneling, an "island". The island is coupled electrostatically to the rest of the circuit by the capacitances C

and C_s whose charges are denoted by Q and Q_s respectively. Although, as we have seen, Q and Q_s are both continuous variables, their difference is the total excess charge of the island. Because charge can enter the island only by tunneling through an insulating barrier, this total charge is a multiple of the electron charge: $Q - Q_s = ne$. Suppose furthermore that the island dimensions are small enough that the electrostatic energy $E_C = e^2/2C_\Sigma$ of one excess electron on the island is much larger than the characteristic energy k_BT of thermal fluctuations. Here, $C_\Sigma = C + C_s$, k_B and T denote the total capacitance of the island, the Boltzmann constant and the temperature, respectively. This Coulomb energy E_C is the other ingredient of controlled electron transfer.

When $U = 0$, n will stay identically zero because the entrance or exit of an electron would raise the electrostatic energy of the island to a level much higher than permitted by thermal fluctuations. As U increases from zero, however, the total energy difference between the $n = 0$ and $n = 1$ state of the whole circuit decreases, because when an electron tunnels to the island the potential drop C_sU/C_Σ partly compensates the electrostatic energy of the island. In fact, a straightforward calculation of the total energy of the circuit yields $\mathcal{E} = E_C(n - C_sU/e)^2 +$ term independent of n. Thus, when $U = e/2C_s$, the $n = 0$ and $n = 1$ states will have the same energy and an electron can tunnel in and out freely. As U is increased further, the $n = 1$ state becomes the lowest energy state. The maximum stability of the $n = 1$ state against fluctuations is reached at $U = e/C_s$ where, as in the case $U = 0$, and $n = 0$, the charge Q vanishes. It is now easy to see that each time the voltage U is increased by e/C_s, the number n of excess electrons of the island is increased by one. If one plots $\bar{n}$, the average of n, as a function of U, one gets the staircase function shown on Fig. 2b. It is therefore possible to control exactly the number of excess electrons of the island by adjusting the voltage U.

As the temperature is increased, the staircase becomes rounded and for temperatures $k_BT \gg E_C$ it approaches the straight dotted line of Fig. 2b. In practise, one can reliably cool tunnel junctions down to 50 mK but not much below. To satisfy $E_C \gg k_BT$, C_Σ must be of the order of or smaller than one femtofarad. This requires the fabrication of junctions with typical areas of 50 nm $\times$ 50 nm and hence the use of nanofabrication techniques. With such low values of capacitance, the typical voltage corresponding to the addition of an electron is of the order of $100\,\mu\mathrm{V} - 1\,\mathrm{mV}$, a value which can be easily controlled electronically. To summarize, tunneling breaks the continuity of the electron fluid into charge packets corresponding to single electrons. The Coulomb energy of excess charges on an island provides a feedback mechanism that regulates the number of electrons tunneling in and out the island. At sufficiently low temperature, the exact number of excess electrons on the island does not fluctuate and can be entirely determined by an externally applied voltage. The quenching of the island

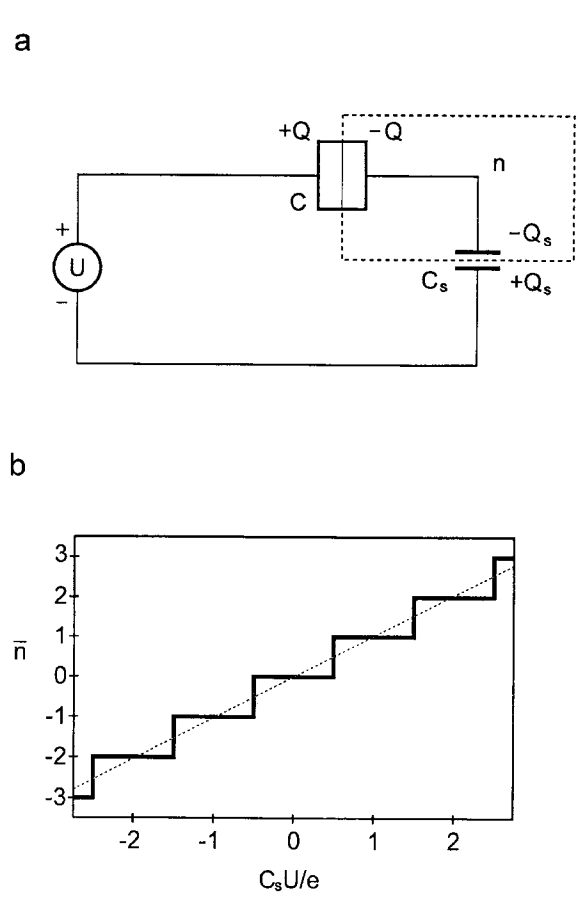

Fig. 2. a) Junction biased by a voltage source U in series with a capacitance C_s. The metal electrode between the junction and the capacitance forms an isolated "island" (box in dashed line) which contains n excess electrons. b) Variation of $\bar{n}$, the average of n as a function of U, when $k_B T \ll E_c$ (full line) and $k_B T \gg E_c$ (dashed line).

charge fluctuations for the "single electron box" (the circuit of Fig. 2a), has been demonstrated experimentally by Lafarge et al. [8].

We have considered so far only thermal fluctuations of the number n. This variable is also subject to quantum fluctuations. In our analysis of the circuit of Fig. 2a, we have neglected the kinetic energy associated with the electron motion under the barrier while tunneling. This energy is very small compared with the Coulomb energy. Perturbative calculations [9,10] show that the quantum fluctuations of n become negligible in the limit $R_t \gg R_K = h/e^2$, where h is Planck's

constant. The constant $R_K \approx 26\text{k}\Omega$ is the resistance quantum. In this course, we will consider tunnel barriers sufficiently opaque that this latter condition is fulfilled. The section on metrological applications (section 2.6) discusses the effect of the quantum fluctuations associated with a finite R_t/R_K ratio.

2.3. *Single electron effects: a brief history*

The combination of the localization of electrons by the tunneling barrier and the Coulomb charging energy give rise to a large class of phenomena which have been called "single electron effects". Decades ago, it was proposed that the variation of the island potential due to the presence of only one excess electron could be large enough to react back on the probability of subsequent tunneling events [11–15]. At that time, the effect could only be observed in granular metallic materials. It was realized that the hopping of electrons from grain to grain could be inhibited at small voltages if the electrostatic energy of a single electron on a grain was much larger than the energy of thermal fluctuations. The interpretation of these pionneering experiments, in which there is an interplay between single-electron effects and random media properties, was complicated by the limited control over the structure of the sample. With modern nanofabrication techniques, it is possible to design metallic islands of known geometry separated by well-controlled tunnel barriers [16]. This led Fulton and Dolan to perform the first unambiguous demonstration of single-electron effects in an island formed by two junctions [17]. Meanwhile, Likharev and coworkers [18,19] had produced detailed predictions of single electron effects in a nanoscale current-biased single junction (this system was also considered in refs. [20] and [21], but only for junctions in the superconducting state) and proposed various applications of the new effects. This current-biased scheme is analogous in some ways to the circuit of Fig. 2a, but with the capacitance replaced by a large resistance. In that case there is no island enforcing charge quantization, because an arbitrarily small amount of charge can flow through the resistance. Only the charge on the junction capacitance would provide the feedback of Coulomb energy on tunneling.

It was later understood that, in general, the quantum electromagnetic fluctuations due to the finite value of the resistance wash out single electron effects in this single-junction no-island system. Only if the value of the resistance is made much larger than the resistance quantum R_K up to frequencies of the order of $e^2/(hC)$ [22–24] can tunneling be Coulomb blocked in the current biased junction system. This effect is the main result of the theory presented in the second part of this course. In spite of the experimental difficulties involved in fabricating the resistance with adequate characteristics, the competition between single electron effects and quantum electromagnetic fluctuations has been observed [25,26]. The single-junction no-island system is certainly of interest as an illustration of

the foundations of the field, but it is not suited for practical applications because getting rid of quantum electromagnetic fluctuations is so difficult experimentally. In what follows, we will resume the discussion of systems that contain at least one island and are thus immune to quantum electromagnetic fluctuations. For general introductions to single-electron effects in normal and superconducting junction systems, see refs. [27–30]. For recent snapshots of the state of current research, see refs. [31,32].

2.4. The single electron transistor

The one-junction one-island circuit of Fig. 2a is the simplest in which single-electron transfer can occur. On the other hand, it cannot produce an externally measurable static current, as the island is a cul-de-sac for electrons. Let us consider the next order of complexity, the two-junction one-island circuit of Fig. 3a [17]. The state of the circuit is now characterized by the two numbers N and N' of electrons having passed through the two junctions. (The increments of N and N' are by convention positive if during tunneling the electron flows in the direction of increasing voltage, and negative otherwise).

It is convenient to introduce the number $n = N - N'$ of excess electrons on the island and the charge flow index $p = (N + N')/2$. The state $(n, p + 1)$ only differs from the state (n, p) in that one electron has been transferred from one terminal of the transport voltage source V to the other. The electrostatic energies of the various capacitances of the circuit are the same. As the precise value of p does not matter here, we will condense the notations (n, p) and $(n, p + 1)$ into (n) and $(n)^*$.

With regard to the total energy of the circuit, which includes the work of the transport voltage, state $(n)^*$ is lower by eV than state (n) and, hence, the circuit has no absolutely stable states. In principle, a steady current I could flow around the loop formed by the two junctions and the transport voltage V. To go from state (n) to state $(n)^*$, however, the circuit must go through state $(n + 1)$ or state $(n - 1)$, because tunnel events occur one at a time. States $(n + 1)$ and $(n - 1)$ differ from state (n) by an electron having tunnelled through the first and second junction, respectively. This is where the single-electron Coulomb energy $E_C = e^2/2C_\Sigma$ comes into play (C_Σ is, as before, the island total capacitance given now by $C_\Sigma = C + C' + C_g$, where C and C' are the two junction capacitances). To simplify the discussion, suppose that $eV \ll E_C$.

When the control "gate" voltage is set at $U = 0$, the energy of states (-1) and (1) will be $E_C - eV/2 \approx E_C$ above the energy of state (0) (see Fig. 3c). At low temperature, this will provide a Coulomb barrier for the transport of electrons around the circuit. In this case the current I should be strictly zero. This situation is called the Coulomb blockade. On the other hand, when the control voltage is

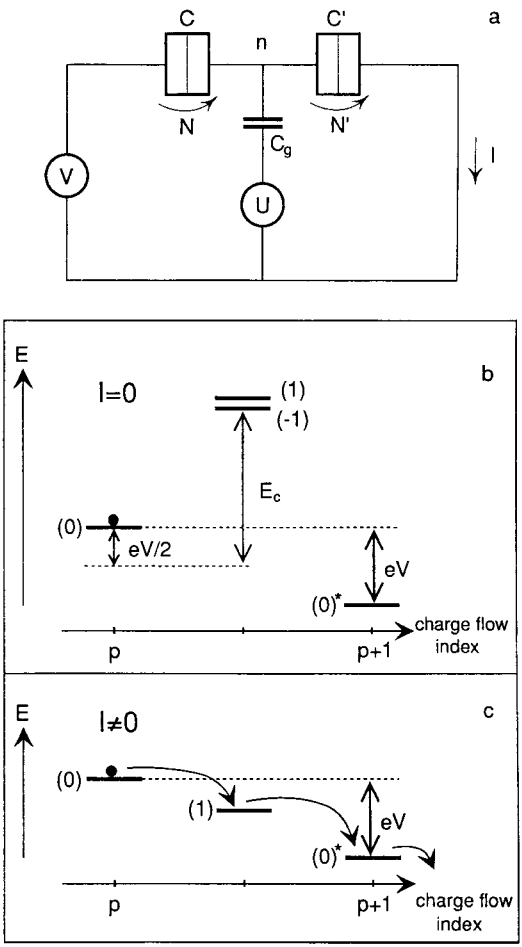

Fig. 3. a) Schematic of single-electron transistor (SET). Energy of the states of the circuit when b) $U = 0$ and c) $U = e/2C_g$. The numbers in parenthesis are the values of the number n of excess electrons on the SET island. The charge flow index is half the sum of the numbers N and N' of electrons that have traversed the junctions. In b) no current can flow through the device: this is the Coulomb blockade.

such that $C_g U \approx e/2$, states (0) and (1) have nearly the same energy (Fig. 3c). As soon as the energy of the (1) state is lowered below that of the (0) state, the $(0) \rightarrow (1)$ transition becomes possible and an electron enters the island through the first junction. If U is such that the energy of the (1) state, although below that of the (0) state, is still above the energy of the $(0)^*$ state, the transition $(1) \rightarrow (0)^*$

takes place and the electron leaves the island through the second junction. Apart from an electron having gone through the device, one is now back to the initial electrostatic state and the cycle can start over again. This cascade of transitions produces a current of order $V/(R_t + R'_t)$ through the device (R_t and R'_t are the tunnel resistances of the two junctions). When U is increased further, the energy of the (1) state goes below the energy of the $(0)^*$ state and one enters a new Coulomb blocked state with one excess electron on the island. The domains that Coulomb blocked states occupy on the U axis when $V \simeq 0$ are in a one-to-one correspondance with the flat portions of the staircase of the electron box (Fig. 2b) and its is easy to show that, at voltages low compared with the Coulomb voltage E_C/e, the current I is maximum when $C_g U = (n + \frac{1}{2})e$.

In practise, a current of the order of 10^9 electrons per second can be switched on and off by the presence or absence of half the electron charge on the gate capacitor, hence the name "single electron transistor" (SET) given to this device. The remarkable charge sensitivity of the SET is unrivalled by other devices: it is six orders of magnitude better than conventional FET electrometers [28]. A possible application is the detection of individual photoinduced electron–hole pairs in semiconductors [33]. But the input capacitance of the SET is, by construction, so tiny that its voltage sensitivity is not high. In this respect, it does not compare favourably with the field effect transistor (FET), the semiconductor device on which most of today's applications of solid-state electronics are based. Furthermore, in the SET the modulation of electron flow by the gate ceases as soon as the bias voltage becomes of the order of the Coulomb gap voltage E_C/e, whereas in the FETs used in digital circuits the modulation of the source-drain current by the gate only saturates at large bias voltages [34]. It is this latter feature which ensures enough voltage gain to compensate for the dispersion in device parameters and which make robust integrated digital circuit design possible with FETs.

An analogy [28] can be drawn between the SET and the dc SQUID with an input coil [35] (see Fig. 4). The d.c. SQUID (superconducting quantum interference device) consists of two Josephson junctions in parallel biased by a static current. In the d.c. SQUID, the output voltage is a periodic function of the current in the input coil, whereas in the SET, the output current is a periodic function of the voltage on the input capacitor. For the d.c. SQUID the period is set by the flux quantum $h/2e$ whereas for the SET the period is set by the charge quantum e. The quantization of flux in the superconducting ring of the SQUID is analogous to the quantization of charge in the island of the SET. It is tempting to speculate that the SET will play the same role for ultra-sensitive electrometry that the d.c. SQUID plays for ultra-sensitive magnetometry. However, the fundamental impossibility of building the charge analogue of the superconducting flux transformer which is so crucial to the use of d.c. SQUIDs may severely limit the use of SETs.

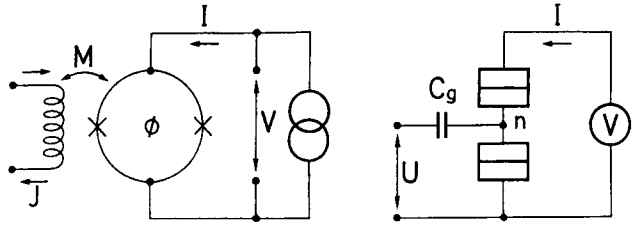

Loop		⟷	Island	
Flux	Φ	⟷	Charge	ne
Bias	I	⟷	Bias	V
Signal	J	⟷	Signal	U
Output	V	⟷	Output	I
Mutual inductance	M	⟷	Capacitance	C_g

Fig. 4. Comparison between the d.c. SQUID (left) and the SET electrometer (right).

The junctions that have been described so far consist in practise of two overlapping metallic films. It is also possible, instead of the three-dimensional gases that conduction electrons form in a metal, to use two-dimensional electron gases which are found in semiconductor heterostructures such as GaAs/GaAlAs. The detailed manifestations of Coulomb blockade have been thoroughly studied in these systems where single-electron effects may coexist with the quantum Hall effect [36].

Finally, Coulomb blockade has been observed with a scanning tunneling microscope (STM) placed over a tiny metallic droplet [37]. The role of the island is played by the droplet. Unfortunately, it has so far been impossible to modulate the gate voltage independently in the droplet-STM systems. On the other hand, very small island dimensions (a few nanometer) can be achieved in this manner, and Coulomb blockade at room temperature has been reported [38]. In principle the island could even be reduced to a single molecule [39].

It is important to note at this point that we describe the state of a circuit such as the SET by discrete variables like n and p, and not by continuous variables like currents and voltages as in classical electronics. What makes nanojunction circuits of fundamental interest is that we must treat them as single, atom-like, quantum systems. Even though we use macrocopic concepts like capacitance, we analyze charge flow in terms of quantum transitions between discrete energy levels of the whole circuit.

2.5. Controlled transfer of charge flowing in an external circuit

Although the principle of the SET involves the electrostatic energy of a single electron on the SET island, the charge flow through this device is not controlled at the single-electron level. The voltage U controls only the average value of the current. The instants at which electrons pass through the device are random, as in a single junction. A control of the charge flow electron by electron would mean that, using the control voltage U, one would make a single electron enter the island from the left junction, hold it in the island for an arbitrary time and finally make it leave the island through the right junction. One could then go continuously from a Coulomb-blocked state with $n = 0$ to a Coulomb-blocked state with $n = 1$. This is not possible with only one island. When the energy of the (1) state dips below the energy of the (0) state, it is necessarily above the energy of the $(0)^*$ state to which it can decay (see Fig. 3c). An electron cannot be made to enter the island through one junction without setting the electrostatic energies so that it is energetically favourable for another electron to leave the island through the other junction.

The control of charge flow at the single-electron level requires at least three junctions [40]. Let us consider the three-junction two-island circuit of Fig. 5a. As in the case of the SET, the state of the circuit can be described using the numbers n_1 and n_2 of excess electrons on each island and the charge flow index given by the third of the algebraic sum of the number of electrons having tunnelled through each junction. Using the condensed notation defined above, (n_1, n_2) and $(n_1, n_2)^*$ denote two states whose charge flow index differ by one, that is, states differing by an electron which has lost energy eV by passing through the entire device.

We suppose $V \ll \min(e/C_{\Sigma 1}, e/C_{\Sigma 2})$ where $C_{\Sigma 1}$ and $C_{\Sigma 2}$ denote the total capacitances of the two islands. The two control voltages U_1 and U_2, applied to the two gate capacitances C_1 and C_2, allow us to change the relative energy of the various states of this circuit. If we set U_1 and U_2 to $e/2C_1$ and $e/2C_2$ respectively, the energies of states $(0,0)$, $(1,0)$, $(0,1)$ and $(0,0)^*$ form a cascade (Fig. 5b). We are in a situation equivalent to the suppression of Coulomb blockade depicted in Fig. 3c, and a stochastic current flows through the device. Because there are three junctions instead of two, there are now two intermediate states $(0,1)$ and $(1,0)$ in the cascade. Each one of these states is coupled to $(0,0)$ or to $(0,0)^*$ but not to both. The lowering of either $(0,1)$ or $(1,0)$ below $(0,0)$ and $(0,0)^*$ stops the stochastic current and puts the circuit in a blocked state.

By modulating U_1 and U_2 with dephased periodic signals, the energy of these intermediate states can be cyclically lowered below that of the $(0,0)$ and $(0,0)^*$ states while avoiding the cascade configuration of Fig. 5b (Fig. 5c–e). One starts from the situation where both $(1,0)$ and $(0,1)$ are above $(0,0)$ and $(0,0)^*$. The

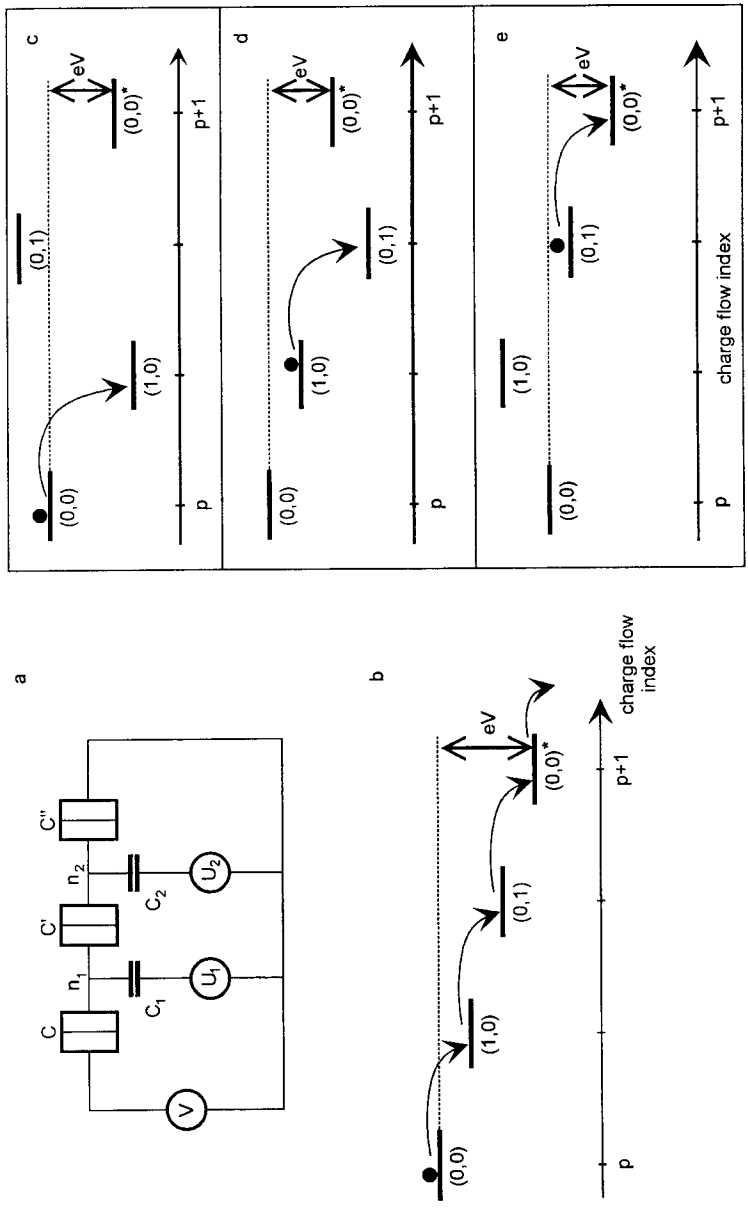

Fig. 5. a) Schematic of the single electron pump. b) Energy states of the circuit when the control voltages U_1 and U_2 are set so that Coulomb blockade is suppressed. c–e) Pumping cycle which transfers one electron around the circuit of a). It is obtained by adding two phase shifted modulation signals on the values of U_1 and U_2 corresponding to b).

circuit is in a blocked state with no excess electrons on the islands. At first, an increase of U_1 lowers $(1,0)$ below $(0,0)$ and $(0,1)$. An electron goes through the left-most junction and the circuit adopts a new blocked state with an extra electron on the first island (Fig. 5c). Then U_2 increases while U_1 decreases: this lowers $(0,1)$ below $(1,0)$ and $(0,0)^*$. A tunnel event consequently takes place through the middle junction and the circuit now adopts a blocked state with an extra electron on the second island (Fig. 5d). Finally U_2 is decreased to its initial value, making $(0,1)$ pass above $(0,0)^*$. An electron goes through the right-most junction and, apart for a charge e having crossed the entire device, the circuit returns to its initial blocked state (Fig. 5e). If the transport voltage V is reversed, the same modulation cycle will continue to carry electrons from left to right, provided the energy difference eV between $(0,0)$ and $(0,0)^*$ stays small compared with the energy excursions of $(0,1)$ and $(1,0)$. The charge now flows in a direction opposite to that imposed by V. Energy conservation is of course not violated. The work done to "charge" the transport voltage source is provided by the control voltage sources. We have therefore nicknamed this three-junction device the single-electron "pump". The pump is reversible: a time-reversed modulation cycle — obtained by reversing the sign of the phaseshift — will transfer electrons from right to left.

The actual operation of a physical device is shown in Fig. 6. We first set U_1 and U_2 to the static values $U_1^{dc} = e/C_1$ and $U_2^{dc} = e/C_2$ corresponding to a maximum zero-voltage conductance (center curve marked "no r.f."). Two periodic signals with the same frequency f but dephased by $\Phi \simeq \pi/2$ are then superimposed on the static components U_1^{dc} and U_2^{dc}. This implements the cycle shown in Fig. 5c–e and a current plateau is observed (see Fig. 6a). One can easily reverse the cycle, leaving all other conditions the same, by changing Φ to $\Phi+\pi$. A current plateau is again observed, with the same absolute value at $V = 0$ but with opposite sign. The height of the plateau is plotted against frequency on Fig. 6b. The relation $I = ef$ is well verified, providing further confirmation that our device does indeed implement the pump principle.

We have seen how two control voltages can transfer electrons one by one in a three-junction device. The transfer of single electron using only one control voltage is possible, but needs at least four junctions. In Fig. 7a we show the schematics of a four-junction three-island circuit which we have nicknamed the "turnstile" [41]. A gate capacitance, with roughly half the value of the capacitance of the junctions, connects the central island to an external control voltage U. Because the gate voltages of the side islands have only to be set to a constant value of zero (in practice, the external gate voltage must be adjusted to compensate for random offset charges [28]), no gate lines have been represented in the figure. The turnstile can be described as a SET with two junctions in the entrance and exit channels. The intermediate islands create energy barriers whose effect is to

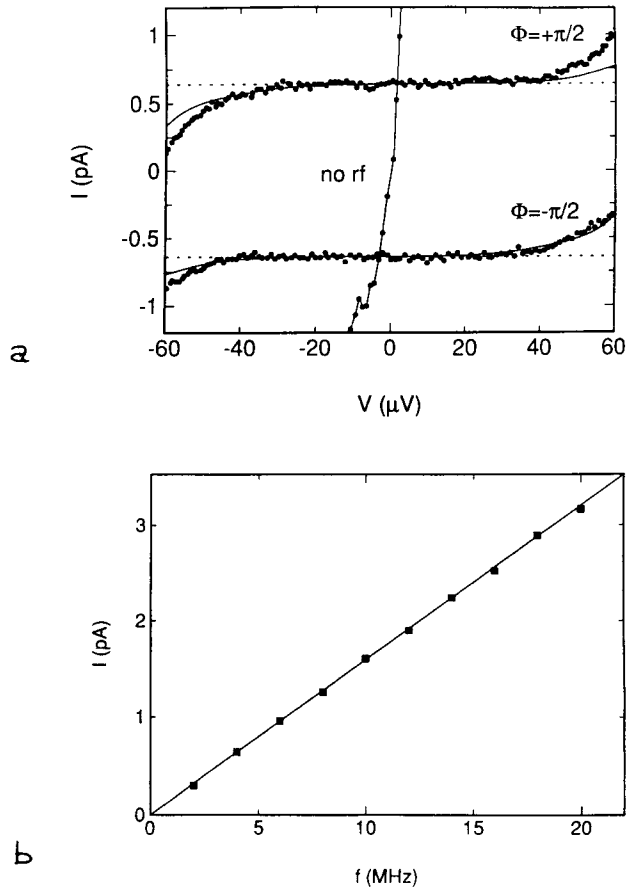

Fig. 6. a) Current–voltage characteristic of the pump with and without a $f = 4$ MHz control voltage modulation. The two modulation signals were phase-shifted by $\Phi \simeq \pm\pi/2$. Dashed lines indicate $I = \pm ef$. Full lines are the result of numerical simulations taking into account quantum fluctuations of the island electron number. b) Current measured at the inflexion point of the current plateau as a function of the frequency f. Full line is $I = ef$.

suppress the stochastic conduction that takes place in the SET for small V, and for U such that $C_g U = e/2$ (see Fig. 7b–d). For these conditions, the circuit can exist in two states characterized by the presence or absence of an extra electron on the central island. Suppose one starts with no electron in the central island. As U is increased, all the energies of the intermediate states decrease, although the state with an electron on the central island remains the lowest of the intermediate states (see Fig. 7b). Consequently, one electron enters the central island. If now

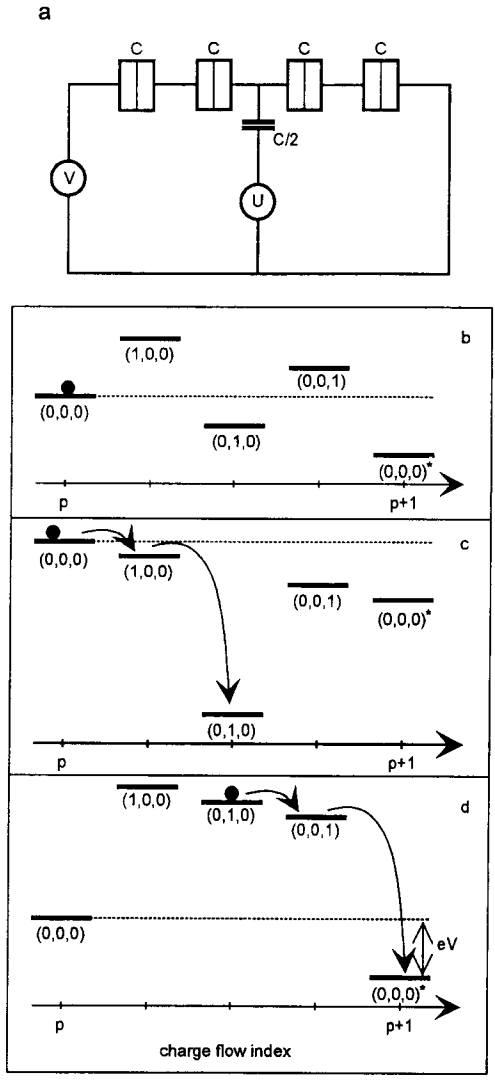

Fig. 7. a) Schematics of single-electron turnstile. b–d) Turnstile cycle which is obtained by modulating the control voltage U and which transfers one electron around the circuit of a).

one decreases U, all the energies of the intermediate states increase and at one point the state with an extra electron on the central island is no longer the lowest of the intermediate states. An electron then leaves the central island (Fig. 7d). It

is easy to see that after one cycle of modulation of U, a charge of one electron has passed through the whole device. Like the pump, the turnstile produces a current $I = ef$, where f is the modulation frequency. Unlike the pump, however, the turnstile is an irreversible device, the sign of the current being imposed by the sign of the bias voltage V.

2.6. *Metrological applications*

We have seen that the pump and the turnstile can produce a current determined only by the frequency f and the quantum of charge e. Because frequencies can be accurately determined, these devices would provide in principle a standard of current. The standard is obtained at present by the combination of the Josephson effect [35], which relates a frequency to a voltage through the flux quantum $\Phi_0 = h/2e$, and the quantum Hall effect discovered by von Klitzing [42], which relates current to voltage through the resistance quantum $R_K = h/e^2$. It is important for metrologists to check if a direct definition of the ampere using the charge quantum e provided by single electron devices is compatible with the "Josephson/Klitzing" definition which combines Φ_0 and R_K. The value of the fine-structure constant $\alpha = e^2/(2h\epsilon_0 c)$, where c and ϵ_0 denote the speed of light and the electrical permittivity in vacuum, is another important metrological issue that would benefit from the new access to the charge quantum provided by single-electron devices [43]. This latter application would not necessitate to measure directly the very low current produced by single-electron devices; one would simply charge a calibrated capacitor with a known number of electrons, and compare its voltage with the Josephson volt.

The first experiments carried out to test the precision of the pump and the turnstile were chiefly limited by the precision of current measurements, and it is important to investigate the intrinsic limitations of the devices. One problem is to ensure that the devices are sufficiently cold while passing current. In that respect the pump principle is better than the turnstile, as the pump is reversible and can operate at zero bias voltage. Theoretical analyses show that the fundamental limitation on the accuracy of the devices is due to co-tunneling events [44] during which several tunnel events take place simultaneously on different junctions. These higher-order processes are a manifestation of the quantum fluctuations of island electron number discussed in section 2.2. Fortunately, it can be demonstrated that the rate of co-tunneling events decreases exponentially with the number of junctions in a device. Detailed calculations have shown that an accuracy better than 10^{-8} in the number of transferred electrons is achievable with a pump with five junctions operating at temperatures of 100 mK or less [45,46]. An important step towards the practical realization of high-accuracy transfer devices is to show experimentally that the number of electrons on an island is well determined when

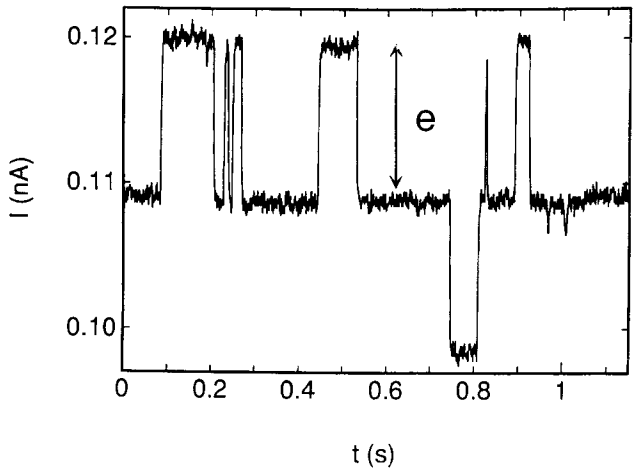

Fig. 8. Time variations of the current through a SET electrometer measuring the charge on an island linked to a charge reservoir through a series of four tunnel junctions. Each jump corresponds to an electron tunneling into or out of the island.

this island is linked to a charge reservoir through four junctions that block the quantum fluctuations of electron number. We have made a direct measurement of the charge of such an island by using a SET electrometer [47]. In Fig. 8 we show single tunneling events in and out the island occurring on a time scale of a tenth of a second. Although this time scale is still shorter than expected theoretically, we believe that if more and smaller junctions were used, the spontaneous tunnel rate could be lowered by two orders of magnitude and thus permit metrological experiments. A breakthrough has recently been made by Martinis et al. who have operated a five-junction pump with a 10^{-6} accuracy [48].

2.7. Single Cooper pair transfer

Up to now we have considered metallic nanojunction circuits in the normal state. For circuits in the superconducting state, one could naively expect that single electron transfer can be transposed into single Cooper pair transfer, e being simply replaced by $2e$. Several features of the superconducting state complicate this direct transposition and early experiments on Cooper pair transfer in superconducting nanojunction circuits showed unexpected results [49–51,8] which we begin to understand in detail only now. Let us go back to our basic circuit, the electron box of section 2.2, and examine the simplest case where only the island is in the superconducting state. The energy of the circuit as a function of the number n of electrons in the island is now $\mathcal{E} = E_C(n - C_sU/e)^2 + (n \bmod 2)\tilde{D} +$

terms independent of n. The first term is the same electrostatic energy as in the normal state, i.e. the electrostatic energy of C and C_s and the work of the voltage source U. The superconducting nature of the island manifests itself in the second term which is the internal energy of the island which we suppose for the moment at $T = 0$. This internal energy depends on n only through its parity, the parameter $\tilde{D}$ denoting the minimum energy of a quasiparticle excitation. Such an odd-even difference is expected for a superconductor, since for an odd number of electrons, one of them cannot be paired and must remain as a quasiparticle excitation [52]. We will discuss this point in more detail in the third part of this course. It is crucial to realize that the energy cost of this remaining quasiparticle excitation coincides with the superconducting energy gap parameter Δ only for an ideal BCS superconductor in zero magnetic field. From the above expression of the circuit energy we can predict the ensemble average $\langle n \rangle$ which we suppose equal to the temporal average $\bar{n}$ measured in the experiment.

In Fig. 9a we show as a function of $C_s U$ the energy of the different n states, for the non-superconducting case $\tilde{D} = 0$. As we have shown in section 2, n will adopt the value of the integer closest to $C_s U/e$, which corresponds to the lowest energy state. We thus get the staircase pattern of Fig. 9b which is identical to the full line curve of Fig. 2b. In Fig. 9c we show the case of a superconducting island such that $\tilde{D} < E_C$. The effect of the odd-even difference is simply to reduce the span of U over which the system will adopt an odd n ground state and, conversely to increase the span of U where an even n state will be favored. We thus get an asymmetric staircase which again has e-steps but which is $2e$-periodic (see Fig. 9d). Finally, in Fig. 9e we show the case of a superconducting island such that $\tilde{D} > E_C$. In that case, for every value of U, the ground state of the circuit always corresponds to an even n, which explains the doubling in Fig. 9f of the height and length of the steps with respect to Fig. 9b.

As we will show in the last part of this course, these theoretical predictions can be extended at temperatures T such that $k_B T \ll E_C$, provided one replaces the zero-temperature odd-even energy difference $\tilde{D}$ by the odd-even *free* energy difference $\tilde{D}(T) = \tilde{D} - k_B T \ln \mathcal{P} + \mathcal{O}(T^2)$ [53,54], where $\mathcal{P} \sim 10^4$, the total number of electron states in the island participating in the superconductivity, is a measure of the degeneracy of the odd ground state with one unpaired electron. In Fig. 10 we show our experimental results for a superconducting aluminium island at $T = 28\,\mathrm{mK}$. In this experiment we vary $\tilde{D}$ by means of a magnetic field applied to the sample. The evolution of the staircase as the field is varied provides a complete confirmation of the predictions of Fig. 9.

A remarkable point which is not completely understood is why the odd-even symmetry breaking which manifests itself in traces b) and c) of Fig. 10 is described so-well by $\tilde{D}(T \to 0) \simeq \Delta_{BCS}$. The superconducting islands are far from ideal: they contain many defects like impurities, grain boundaries and sur-

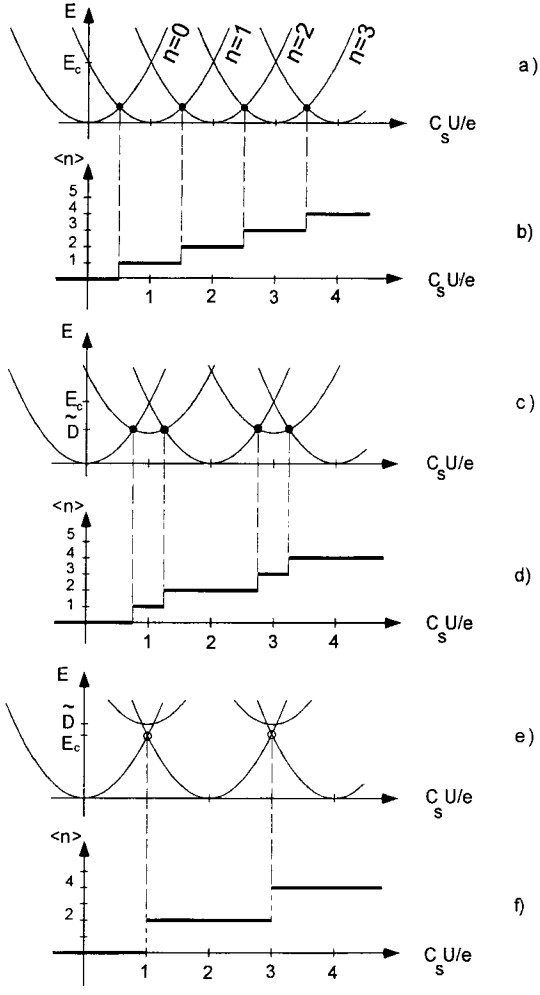

Fig. 8. Total energy of the electron box (Fig. 2a) as a function of the polarization $C_s U/e$, for several values of the excess number n of electrons in the island, in the non-superconducting state (a) and superconducting state (c, e). E_c is the electrostatic energy of one excess electron on the island for $U = 0$. The minimum energy for odd n is $\tilde{D}$ above the minimum energy for even n. Panels c and e differ by the relative magnitude of $\tilde{D}$ and E_c. The black dots correspond to level crossings where a single electron tunnels into and out of the island. The hollow circles correspond to level crossings where the only allowed process is the simultaneous tunnelling of two electrons into the island to form a pair (Andreev process). The equilibrium value $\langle n \rangle$ versus $C_s U/e$ is shown in the non-superconducting (b) and superconducting (d, f) states, at $T = 0$. The Andreev process is shown in f) by a vertical dashed line to distinguish it from the single electron tunneling process shown in b) and d) by a vertical continuous line.

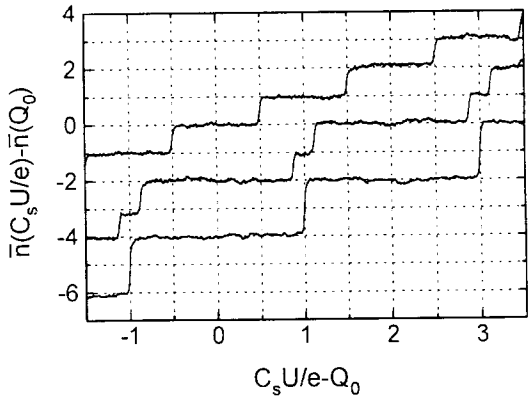

Fig. 10. Variations of the average charge of the island, in units of e, with the polarization C_sU/e, at $T = 28$ mK, for 3 values of the magnetic field H applied to the sample. For the top trace ($H = 0.2$ T) the island is non-superconducting. For the middle ($H = 0.05$ T) and bottom ($H = 0$) traces the island is superconducting. For clarity, the middle and bottom traces have been offset vertically by 2 and 4 units, respectively. The symbol Q_0 refers to the offset charge on the island, an uncontrolled parameter which can be taken as a constant during the duration of measurement, even if it is found to be drifting on the time scale of a few hours.

face states. Apparently, none of these defects provides available states near the Fermi energy for an unpaired electron, which could ruin ideal BCS behavior. However, at the time of this writing, the samples in superconducting box experiments are often found to be described by $\tilde{D} < \Delta_{BCS}$ when both sides of the junction are superconducting. A possible explanation is that in the expression for the odd-even free energy difference $\tilde{D}(T)$, the temperature that enters is the temperature of the quasiparticles, not the phonon temperature. In an all-superconducting circuit at low temperature, quasiparticles can have a very long lifetime and thus, it is possible that the remaining out-of-equilibrium quasiparticles suppress partly the odd-even asymmetry. Having normal metal on one side of the junction provides an efficient way of relaxing out-of-equilibrium quasiparticles, since they can diffuse into the normal metal but not out.

It is also important to note that when both sides of the junction are superconducting, the Andreev process of Fig. 9e, by which two electrons from the normal side tunnel coherently to form a pair in the island, is replaced by Josephson tunneling. In contrast with single electron tunneling or Andreev two-electron tunneling which are irreversible processes characterized by a rate, Josephson tunneling is a reversible process characterized by a macroscopic coupling energy $E_J \sim \Delta(R_K/R_t)$. When $k_BT \ll E_J$, the superconducting electron box polarized at $C_sU/e = 1$ should be in the macroscopic coherent superposition of charge

states ($\mid n = 0 > + \mid n = 2 >)/\sqrt{2}$ [55]. This has been indirectly observed in recent experiments in which the critical current of the superconducting SET has been measured as a function of gate voltage [56,57]. In particular, the experiment of Joyez *et al.* [57] demonstrates that the naive picture of single Cooper pair transfer in nanojunction circuits can hold only if the characteristic energies of the superconductors are set properly, i.e. $\tilde{D}(T \to 0) \simeq \Delta_{BCS}(T) > E_c \gg E_J \gg k_B T$.

2.8. Future prospects

It has been suggested [27,28] that single-electron devices might find applications in digital electronics. A single electron would code for one bit, obviously the most economical way to store information. In fact, the electron pump is already very similar to the shift registers found in computers. The SET would be the building block of this "single electronics". A problem, however, is that metallic SETs made using today's technology have no "engineer gain": one transistor can barely feed one other transistor in the chain of signal processing, once the dispersions on parameters are accounted for. And no one understands how to get rid of random offset charges [28] which at present ruin any attempt to have more than a few transistors on one chip. In semiconductor devices, single-electron effects may even appear to be a nuisance because they imply that the electrons go through the dots or channels one at a time, slowing down the conventional FET operation. The main benefit of understanding single-electron effects in semiconductor nanotechnology may be just to provide the knowledge to fight them efficiently.

The real virtue of single-electron devices, as far as industrial applications are concerned, is that they teach us how to produce digital functions using only tunneling and the Coulomb interaction, basic ingredients that are available down to the molecular level. In the to be developed "molecular electronics" technology [58], basic time constants are very short, there is no dispersion in the parameters of individual components and there are few electrons to work with anyway. There, the principles underlying the devices that have been discussed in this article may be fruitfully implemented. The ultimate computer imagined by Feynman [59], in which elementary information is carried by a single electron on a single atom, would then cease to be a mere theoretical construction and become a reality.

3. Quantum dynamics of tunnel junction circuits

3.1. Introduction

We have mentioned in the first part of this course that electron transfer in ultrasmall tunnel junction circuits is governed by the total energy of the whole cir-

cuit including the work of voltage sources. Indeed, these circuits have been treated in the preceding chapter as if they were large molecules, an electron transfer corresponding to a transition between two many-body energy levels of the molecule. This approach differs radically from classical circuit theory, in which the time evolution of a circuit is governed by a set of "local" equations: the current in a given branch of the circuit depends only on the generalized flux associated with this branch — which is defined as the time integral of the voltage across the branch — and its time derivatives. The aim of this chapter is to present the full quantum theory of tunnel junction circuits, in which the global and the local treatments correspond to two particular approximations, valid in two opposite limits.

3.2. *Conduction in tunnel junction circuits*

A tunnel junction circuit, such as the circuits of Figs. 3a, 5a and 7a, can be described formally as a network of tunnel junctions, pure capacitors and voltage sources with internal impedance. Each junction j is characterized by a tunnel resistance R_{tj} and capacitance C_j, while each pure capacitor i is characterized only by a capacitance C_i. A tunnel junction must be thus thought as being composed of two irreducible elements in parallel: a tunnel element and a capacitance (see Fig. 11a).

The dynamical state of the circuit is described *a priori* by two sets of degrees of freedom: the integers N_j describing how many electrons went through each junction j prior to a particular instant of time and the continuous electrical variables which are the charges Q_j and Q_i stored on capacitances C_j and C_i and the degrees of freedom of the internal impedances of the sources. The set of numbers $\{N_1, N_2, \ldots N_j, \ldots\}$ is called the configuration of the circuit and plays a particular role. For practical circuits, the average rate of charge transfer through the tunnel barriers is much slower than the rate at which the continuous charge redistributes itself on the various capacitances of the circuit. In other words, the time scale of variations of the Q's is much shorter than the time scale of variations of the N's. The dynamics of tunnel junction circuits on the long time scale can therefore be thought of as a sequence of transitions $\{N_1, N_2, \ldots N_j, \ldots\} \rightarrow \{N'_1, N'_2, \ldots N'_j, \ldots\}$ in configuration space, the Q's and the degrees of freedom of the sources evolving rapidly to their electrostatic equilibrium values between two transitions. This relaxation is due to the internal impedances of the sources, which have non-zero real parts and provide dissipation. The relative opaqueness of the tunnel barriers to charge transfer ($R_j \gg h/e^2$) further simplifies the analysis of electron conduction processes. To first order, we need only to consider processes in which only one of the N's vary, i.e. processes such as $\{N_1, N_2, \ldots N_j, \ldots\} \rightarrow \{N_1, N_2, \ldots N_j \pm 1, \ldots\}$. We call these processes single tunneling events. Multiple tunneling events — also called co-tunneling

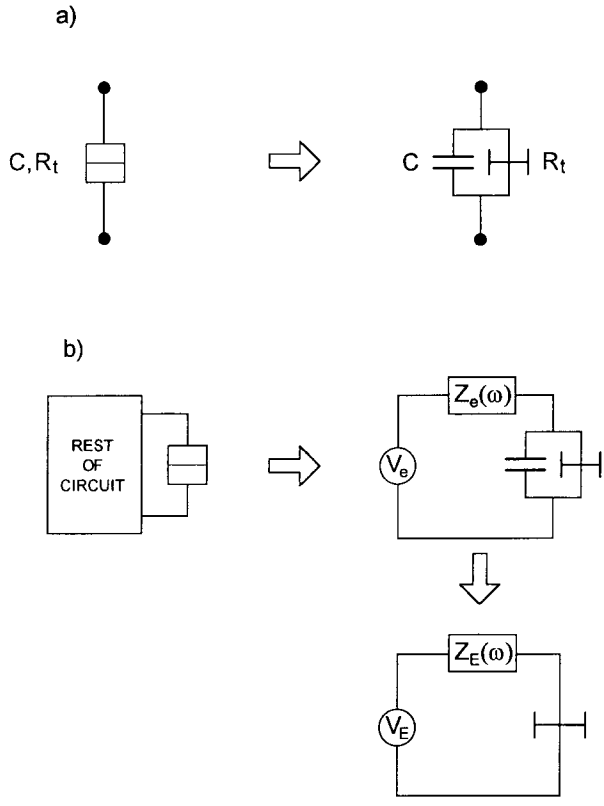

Fig. 11. a) A tunnel junction can be decomposed into two irreducible elements: a capacitance C and a tunnel resistance R_t. b) A junction imbedded in an arbitrary circuit sees a dipole element which can be modelled as a voltage source in series with a frequency dependent impedance. It is convenient to introduce the dipole element seen by the tunnel element itself. This dipole includes the capacitance of the junction.

events — are processes in which several N's vary simultaneously. As mentioned in section 2.6, they occur much less frequently than single tunneling events (when the latter are allowed, of course) and can be neglected in a first approximation. The single electron tunnel process $\{N_1, N_2, \ldots N_j, \ldots\} \rightarrow \{N_1, N_2, \ldots N_j \pm 1, \ldots\}$ occurs at random in a Poissonian fashion and is characterized by a rate $\Gamma_j^{\pm}$ which depends on the initial configuration $\{N_1, N_2, \ldots N_j, \ldots\}$ and on the values of the voltage sources. Electron conduction in a tunnel junction circuit is thus essentially a random sequence of single tunneling events which forms a Markov process between nearest neighbours in configuration space.

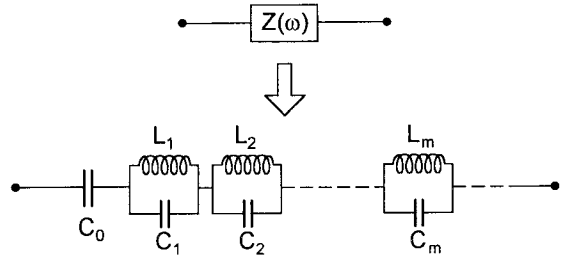

Fig. 12. A general impedance $Z(\omega)$ can be represented by an infinite series of LC oscillators. The series capacitance C_0 is infinite if $\omega Z(\omega) \to 0$ when $\omega \to 0$.

The calculation of the statistical average of the current through the various branches of the circuit — which correspond to the classical notion of the instantaneous current through a branch — reduces to the calculation of the tunnel rates $\Gamma_j^{\pm}$.

3.3. Description of the electromagnetic environment

Since we only deal with one tunnel event at a time, only the non-linear behavior of the junction on which the single tunneling event takes place needs to be considered.

Consequently, from the point of view of this junction, we can treat the rest of the circuit as a linear circuit. We know from circuit theory (Thévenin's theorem) that a general linear circuit viewed from a dipole element such as a junction can be modelled as a series combination of an effective voltage source V_e and an effective frequency-dependent impedance $Z_e(\omega)$ (see Fig. 11b), although the computation of V_e and $Z_e(\omega)$, which depend in general on all the elements of the circuit, can be tedious. In the literature, the V_e and $Z_e(\omega)$ combination is often referred to as the electromagnetic environment of the junction. As we will see in the quantum calculation of the tunnel rate $\Gamma_j^{\pm}$, it is preferable to lump into V_e and $Z_e(\omega)$ the junction capacitance C_j. This defines a V_{E} and $Z_{\mathrm{E}}(\omega)$ environment in parallel with the tunnel element (see Fig. 11b), such that $Z_{\mathrm{E}}^{-1}(\omega) = Z_e^{-1}(\omega) + iC_j\omega$ and $V_{\mathrm{E}} = [C_e/(C_e + C_j)]\, V_e$, where $C_e = \left[\lim_{\omega \to 0} [i\omega Z_e(\omega)]\right]^{-1}$.

Although the dissipation described by $\mathrm{Re}\,[Z_{\mathrm{E}}(\omega)]$ can be non-electromagnetic in origin, being due for example to electron–phonon collisions, the linearity of the circuit warrants that, as far as its influence on the junction is concerned, $Z_{\mathrm{E}}(\omega)$ can be represented as an infinite series of LC circuits [60] (see Fig. 12).

Mathematically, this corresponds to defining a series of capacitances C_m $(m \in$

$\{0, 1, 2, \ldots\}$) and inductances L_m ($m \in \{1, 2, \ldots\}$) from the relations:

$$Z_{\mathrm{E}}(\omega) = \lim_{\eta \to 0^+} \lim_{\epsilon \to 0} \left\{ \frac{C_0^{-1}}{i\omega} + \sum_{m=1}^{\infty} \left[\frac{\frac{1}{2} C_m^{-1}}{i(\omega - \omega_m) + \eta} + \frac{\frac{1}{2} C_m^{-1}}{i(\omega + \omega_m) + \eta} \right] \right\} \tag{3.1}$$

$$\omega_m = m\epsilon = \sqrt{\frac{1}{L_m C_m}} \tag{3.2}$$

In this representation, the real part of the impedance corresponds to the spectral density of an infinite set of LC resonant modes:

$$\mathrm{Re}\left[Z_{\mathrm{E}}(\omega > 0)\right] = \frac{\pi}{2} \lim_{\epsilon \to 0} \sum_{m=1}^{\infty} Z_m \omega_m \delta(\omega - \omega_m) \tag{3.3}$$

where the mode impedance Z_m is given by

$$Z_m = \sqrt{\frac{L_m}{C_m}} \tag{3.4}$$

Note that the pole at $\omega = 0$ which is excluded from expression (3.3) is present only if there is at least one junction or a pure capacitor in series with the junction in the original circuit. If, on the other hand, there is a conducting path around the circuit through which the charge accumulated on the junction capacitance can relax to zero, then $C_0^{-1} = 0$.

As we will see in the following, it is important to distinguish the d.c. parameters of the environment, V_{E} and C_0^{-1}, from the a.c. ones described by the set C_m and L_m ($m = 1, 2, \ldots \infty$) , or equivalently, by the function $Z'_{\mathrm{E}}(\omega) = Z_{\mathrm{E}}(\omega) - C_0^{-1}/i\omega$. Suppose we start at $t = 0$ with an initial equilibrium situation in which there is a charge Q_0 on the capacitance C_0, resulting from the previous electron transfers. There will be an initial voltage $v(t = 0) = V_{\mathrm{E}} + C_0^{-1} Q_0$ across the environment viewed from the tunnel element. If we replace the tunnel element by a current source injecting in the environment a current pulse $-e\delta(t)$, the resulting voltage $v(t > 0)$ across the environment will be given by $v(t > 0) = V_{\mathrm{E}} + C_0^{-1}(Q_0 - e) - e\mathcal{R}(t)$ where $\mathcal{R}(t)$ is the charge relaxation function

$$\mathcal{R}(t) = \frac{1}{\pi} \int_{-\omega}^{+\omega} d\omega \exp(i\omega t) \mathrm{Re}\left[Z_{\mathrm{E}}(\omega)\right] \tag{3.5}$$

The charge relaxation function $\mathcal{R}(t)$ is such that $\mathcal{R}(t \to 0^+) = C_j^{-1} - C_0^{-1}$. In practise $\mathrm{Re}\left[Z_{\mathrm{E}}(\omega)\right]$ is a continuous function and has the property $\mathcal{R}(t \to \infty) = 0$. Thus $v(t \to \infty) = V_{\mathrm{E}} + C_0^{-1}(Q_0 - e)$.

One may wonder why the junction environment is not treated by the full Maxwell's equations involving three-dimensional field quantities. The answer is that

it is sufficient to deal only with lumped element quantities like voltages, currents and impedances because the dimensions of the tunnel junctions we consider are always much smaller than the wavelength of electromagnetic radiation at the relevant energy scales.

3.4. *The total electrostatic energy $\mathcal{E}$*

As we will see in the following, an important quantity which enters in the dynamics of tunneling is $\Delta\mathcal{E}$, the difference in the total electrostatic energy of the circuit, including the work done by the voltage sources, before and after tunneling, when the charge relaxation function has decayed to zero.

This energy difference can be computed from the effective circuit viewed from the junction. We have

$$\Delta\mathcal{E} = \frac{(Q_0 - e)^2}{2C_0} - eV_{\mathrm{E}} - \frac{Q_0^2}{2C_0} = -e\frac{Q_0 + C_0V_{\mathrm{E}} - e/2}{C_0} \tag{3.6}$$

Note that Q_0 depends on previous tunnel events and has to be computed, like C_0 and V_{E}, from the elements of the whole circuit. It is often easier to obtain $\Delta\mathcal{E}$ from the expression of $\mathcal{E}$. This latter quantity can be directly computed from the set $\{n_1, n_2, \ldots n_\alpha, \ldots\}$ describing the number of excess electrons on the islands and from the set $\{p_1, p_2, \ldots p_i, \ldots\}$ describing the number of electrons having passed through the voltage sources V_i directly connected between a junction and ground. These sets of numbers can themselves be easily deduced from the junction electron configuration $\{N_1, N_2, \ldots N_j, \ldots\}$.

$$\mathcal{E} = \frac{1}{2}\sum_{\alpha,\beta}\left[\mathsf{C}^{-1}\right]_{\alpha\beta}\left(-n_\alpha e + \widetilde{Q}_\alpha\right)\left(-n_\beta e + \widetilde{Q}_\beta\right) - \sum_i p_i e V_i + \mathcal{E}_0 \tag{3.7}$$

In this last expression, C^{-1} is the inverse of the matrix whose off-diagonal elements are the opposite $-C_{\lambda\mu}$ of the island-island capacitances and whose diagonal elements are the total self-capacitances $C_{\Sigma\lambda}$ of the islands. The charge of the electron is by definition $-e$. The quantity $\widetilde{Q}_\alpha = \sum_s C_{\alpha s}U_s$ is the bias charge of island α which depends on the voltage sources U_s connected between island and ground through the island-source capacitances $C_{\alpha s}$. Finally $\mathcal{E}_0$ is the initial charging energy of the circuit whose terms are independent of the n's and the p's. Expression (3.7) generalizes to an arbitrary circuit the expression of the energy of the single electron box given in section 2.2.

3.5. Quantum mechanical treatment of the junction coupled to its electromagnetic environment

The microscopic degrees of freedom of the junction itself can be described with the annihilation operators $a_{l\sigma}$ and $b_{r\sigma}$ for the Fermi-liquid quasiparticle levels on the left and right side of the junction respectively. The symbols l and r denote the energy level index and $\sigma \in \{\uparrow, \downarrow\}$. These quasiparticle levels can be defined only if their energies lie in the neighbourhood of the Fermi energy E_F and the description in terms of single particle operators is valid only for temperatures $T \ll E_F/k_B$. These operators obey the standard fermion operators anticommutation relations:

$$\left\{a_{k\sigma}, a^{\dagger}_{k'\sigma'}\right\} = \delta_{kk'}\delta_{\sigma\sigma'} \tag{3.8}$$

$$\{a_{k\sigma}, a_{k'\sigma'}\} = 0 \tag{3.9}$$

$$\left\{a^{\dagger}_{k\sigma}, a^{\dagger}_{k'\sigma'}\right\} = 0 \tag{3.10}$$

We can define the number of quasiparticles on the left and right side of the junction from

$$N_l = \sum_{l\sigma \in \mathcal{L}} a^{\dagger}_{l\sigma}\, a_{l\sigma} \tag{3.11}$$

$$N_r = \sum_{r\sigma \in \mathcal{R}} b^{\dagger}_{r\sigma}\, b_{r\sigma} \tag{3.12}$$

Here $\mathcal{L}$ and $\mathcal{R}$ refer to sets of quasiparticles levels lying near the Fermi level. The difference between the number of quasiparticles on the left and right side of the junction is related to the number of electrons that went through the junction by

$$N = \frac{1}{2}\,(N_r - N_l) + \mathcal{N}_{\mathrm{ref}} \tag{3.13}$$

where $\mathcal{N}_{\mathrm{ref}}$ is a constant depending only on the definition of the sets $\mathcal{L}$ and $\mathcal{R}$. The variable N is the macroscopic degree of freedom of the tunnel element.

As far as the environment described by V_{E} and $Z_{\mathrm{E}}(\omega)$ is concerned, we need only to take into account its macroscopic degrees of freedom. They are the degrees of freedom of the LC modes corresponding to the poles of $Z_{\mathrm{E}}(\omega)$ given in expression (3.1). The most convenient representation here is to take as degrees of freedom the fluxes ϕ_m in the inductances L_m and the conjugated charges q_m. The variables ϕ_m and q_m are defined in terms of the voltage $v^L_m(t)$ across L_m and the current $i^L_m(t)$ through L_m by

Table 1

Comparison between electrical and mechanical oscillator

Electrical LC oscillator	Mechanical spring-mass oscillator
Flux ϕ	Coordinate x
Charge q	Momentum p
Capacitance C	Mass m
Voltage q/C	Velocity p/m
Inductance L	Inverse spring constant k^{-1}
Current ϕ/L	Force kx
Frequency $\omega = 2\pi\,(LC)^{-1/2}$	Frequency $\omega = 2\pi\sqrt{k/m}$
$[\phi, q] = i\hbar$	$[x, p] = i\hbar$

$$\phi_m(t) = \int_{-\infty}^{t} v_m^L(\tau)d\tau \tag{3.14}$$

$$q_m(t) = \int_{-\infty}^{t} i_m^L(\tau)d\tau \tag{3.15}$$

It can be shown that, in a general circuit consisting of inductances and capacitances, the equations of evolution correspond to Hamilton equations in which the ϕ's are position coordinates and the q's are momentum coordinates (see Table 1 above).

The corresponding quantum-mechanical operators obey therefore the commutation relations

$$\left[\widehat{\phi}_m, \widehat{q}_{m'}\right] = i\hbar\delta_{mm'} \tag{3.16}$$

$$\left[\widehat{\phi}_m, \widehat{\phi}_{m'}\right] = 0 \tag{3.17}$$

$$\left[\widehat{q}_m, \widehat{q}_{m'}\right] = 0 \tag{3.18}$$

In the following , we will drop the hat on the operators since using the same symbol for the classical and quantum variable will not lead to any confusion.

We can also introduce the electrical variables of the capacitors C_m where $m \in \{1, 2, \ldots\}$.

$$\Phi_m(t) = \int_{-\infty}^{t} v_m^C(\tau)d\tau \tag{3.19}$$

$$Q_m(t) = \int_{-\infty}^{t} i_m^C(\tau) d\tau \tag{3.20}$$

From Kirchhoff's laws applied to the circuit of Fig.12 we see that the Φ's and Q's are related to the ϕ's and q's by

$$\Phi_m(t) = \phi_m(t) \tag{3.21}$$

$$Q_m(t) = Q_0 - q_m(t) \tag{3.22}$$

where the parameter Q_0 denotes the constant charge on the capacitor C_0.

We assume from now on that the macroscopic degrees of freedom q's and the ϕ's commute with the microscopic degrees of freedom $a_{l\sigma}$ and $b_{r\sigma}$. This hypothesis is justified in a system with a large number of electrons since the contribution of a single electron state to an operator describing the collective motion of all the electrons is negligible.

If the tunnel element was absent, the dynamics of the environment would be described by the hamiltonian

$$\mathcal{H}_{\mathrm{E}} = \sum_{m=1}^{\infty} \left[\frac{\phi_m^2}{2L_m} + \frac{(q_m - Q_0)^2}{2C_m} \right] + \frac{Q_0^2}{2C_0} + Q_0 V_E \tag{3.23}$$

The term $\phi_m^2/2L_m$ describes the magnetic energy stored in the inductor L_m. The term $(q_m - Q_0)^2/2C_m$ describes the electrostatic energy stored in the capacitor C_m expressed in terms of the variable conjugate to ϕ_m. The last two terms of $\mathcal{H}_{\mathrm{E}}$ have been included only to account for the constant energy due to the offset charge Q_0 on the capacitance C_0. They play no role in the dynamics of the system.

The dynamics of the coupled junction + environment system can be obtained from the following hamiltonian

$$\mathcal{H} = \mathcal{H}_{qp} + \mathcal{H}_t + \mathcal{H}'_{\mathrm{E}} \tag{3.24}$$

where $\mathcal{H}_{qp}$ is the hamiltonian describing the Fermi-liquid quasiparticle excitations of the left and right electrode of the junction and $\mathcal{H}_t$ the tunnel hamiltonian which couples the quasiparticle excitations of the left and right electrodes. The part $\mathcal{H}'_{\mathrm{E}}$ denotes the modified hamiltonian of the electromagnetic environment. It takes into account the coupling between the quasiparticle and electromagnetic degrees of freedom by the replacement $Q_0 \rightarrow Q_0 - Ne$ (we count N as increasing when a tunnel event decreases the capacitor charge).

These three pieces $\mathcal{H}_{qp}$, $\mathcal{H}_t$ and $\mathcal{H}'_{\mathrm{E}}$ are given by

$$\mathcal{H}_{qp} = \sum_{l\sigma} \epsilon_l \, a_{l\sigma}^{\dagger} \, a_{l\sigma} + \sum_{r\sigma} \epsilon_r \, b_{r\sigma}^{\dagger} \, b_{r\sigma} \tag{3.25}$$

$$\mathcal{H}_t = \sum_{rl\sigma} t_{rl\sigma}\, b^\dagger_{r\sigma}\, a_{l\sigma} + \text{h.c.} \tag{3.26}$$

$$\mathcal{H}'_{\mathrm{E}} = \sum_{m=1}^{\infty} \left[\frac{\phi_m^2}{2L_m} + \frac{(q_m - Q_0 + Ne)^2}{2C_m} \right] + \frac{(Q_0 - Ne)^2}{2C_0} + (Q_0 - Ne)V_E \tag{3.27}$$

The form of $\mathcal{H}'_{\mathrm{E}}$ shows that the effect of the tunnel hamiltonian is to shift by e the charge on each environmental LC oscillator.

It is useful to make a change of representation

$$\widetilde{\mathcal{H}} = U^\dagger \mathcal{H} U \tag{3.28}$$

with the unitary operator

$$U = \exp\left[-i\frac{e}{\hbar}\phi N\right] \tag{3.29}$$

where

$$\phi = \sum_{m=1}^{\infty} \phi_m \tag{3.30}$$

Using the algebraic relations

$$\exp\left(i\frac{e}{\hbar}\phi_m\right) Q_m \exp\left(-i\frac{e}{\hbar}\phi_m\right) = Q_m - e \tag{3.31}$$

$$\exp\left(+i\Lambda a^\dagger a\right) a \exp\left(-i\Lambda a^\dagger a\right) = a \exp\left(-i\Lambda\right) \tag{3.32}$$

and the relations (3.21) and (3.22), we find that the new hamiltonian $\widetilde{\mathcal{H}} = \widetilde{\mathcal{H}}_{qp} + \widetilde{\mathcal{H}}_t + \widetilde{\mathcal{H}'}_{\mathrm{E}}$ is given by

$$\widetilde{\mathcal{H}}_{qp} = \sum_{l\sigma} \epsilon_l\, a^\dagger_{l\sigma}\, a_{l\sigma} + \sum_{r\sigma} \epsilon_r\, b^\dagger_{r\sigma}\, b_{r\sigma} \tag{3.33}$$

$$\widetilde{\mathcal{H}}_t = \sum_{rl\sigma} t_{rl\sigma}\, b^\dagger_{r\sigma}\, a_{l\sigma} \exp\left(i\frac{e}{\hbar}\Phi\right) + \text{h.c.} \tag{3.34}$$

$$\widetilde{\mathcal{H}'}_{\mathrm{E}} = \sum_{m=1}^{\infty} \left[\frac{\Phi_m^2}{2L_m} + \frac{Q_m^2}{2C_m} \right] + \frac{(Q_0 - Ne)^2}{2C_0} + (Q_0 - Ne)V_{\mathrm{E}} \tag{3.35}$$

The hamiltonian $\widetilde{\mathcal{H}}$ operates inside a Hilbert space in which, in absence of $\widetilde{\mathcal{H}}_t$, the quasiparticles are only coupled to the d.c. potential V_{E} and the offset charge Q_0. The phase factor in the tunnel hamiltonian $\widetilde{\mathcal{H}}_t$ ensures that each time an electron goes through the junction and creates a quasielectron–quasihole pair

across the junction, the charge Q_m of every oscillator capacitor in the environment is shifted by e. This phase factor is absent in standard tunneling rate theories which consider that the environment can be treated as an ideal voltage bias.

The $\mathcal{H}$ representation is well suited for problems in which one needs to treat the tunnel hamiltonian to high orders, but is satisfied with the environment treated in a perturbative way. On the other hand, the $\widetilde{\mathcal{H}}$ representation is better suited for problems in which the tunnel hamiltonian needs only to be treated to the lowest significant order, but in which the environment needs to be treated to all orders. Since in this chapter we are mostly interested in the influence of a general environment on the tunneling process through an opaque junction, we have to use the $\widetilde{\mathcal{H}}$ representation, as we will show now.

The parameter that specifies how strongly an environmental mode m is coupled to the quasiparticles can be obtained by expressing Φ_m and Q_m in terms of the "photon" operators c_m and $c_m^\dagger$ such that $\left[c_m, c_m^\dagger\right] = 1$.

$$\Phi_m = \sqrt{\frac{\hbar Z_m}{2}}\left(c_m^\dagger + c_m\right) \tag{3.36}$$

$$Q_m = i\sqrt{\frac{\hbar}{2Z_m}}\left(c_m^\dagger - c_m\right) \tag{3.37}$$

With these photon operators expressions (3.34) and (3.35) become

$$\widetilde{\mathcal{H}}_t = \sum_{rl\sigma} t_{rl\sigma}\, b_{r\sigma}^\dagger\, a_{l\sigma} \exp\left[i\sum_{m=1}^{\infty}\sqrt{\frac{\pi Z_m}{h/e^2}}\left(c_m^\dagger + c_m\right)\right] + \text{h.c.} \tag{3.38}$$

$$\widetilde{\mathcal{H}'}_{\mathrm{E}} = \sum_{m=1}^{\infty}\hbar\omega_m\left(c_m^\dagger c_m + 1/2\right) + \frac{\left(Q_0 - Ne\right)^2}{2C_0} - \left(Q_0 - Ne\right)V_{\mathrm{E}} \tag{3.39}$$

We see that the coupling of a mode to the tunneling electrons involves the ratio η of the mode impedance Z_m to the impedance quantum $R_K = h/e^2$. Now, in the case where the environment behaves at low frequencies like a resistor R, a quite generic situation if there is no capacitor or other junction in series with the junction we consider, expression (3.3) shows that the ratio η is proportional to $\frac{1}{m\epsilon}R/R_K$ and thus diverges as $\epsilon \longrightarrow 0$. A non-perturbative quantum-mechanical treatment of the low frequency environment oscillators is clearly needed in this case, which is of particular relevance to experiments in which one measures the current–voltage relationship of a single tunnel junction.

3.6. Calculation of tunnel rates

The tunnel rate Γ_j^+ can be expressed as a function of $\Delta\mathcal{E}$ and $\mathrm{Re}[Z(\omega)]$. We start by using Fermi's Golden Rule:

$$\Gamma_j^+ = \sum_{I,F} p_I \Gamma_{I\to F} \tag{3.40}$$

where

$$\Gamma_{I\to F} = \frac{2\pi}{\hbar} \left| \langle F \mid \widetilde{\mathcal{H}}_t \mid I \rangle \right|^2 \delta(E_I - E_F) \tag{3.41}$$

In these expressions, $\mid I\rangle$ and $\mid F\rangle$ denote initial and final states of the junction + environment system before and after tunneling, E_I and E_F the corresponding energies and p_I the probability of finding the system in state $\mid I\rangle$. The states $\mid I\rangle$ and $\mid F\rangle$ can be expressed as products of quasiparticle states and environmental photon states:

$$\mid I\rangle = \mid \Psi_I^{qp}\rangle \mid \Psi_I^{ph}\rangle \tag{3.42}$$

$$\mid F\rangle = \mid \Psi_F^{qp}\rangle \mid \Psi_F^{ph}\rangle \tag{3.43}$$

$$\mid \Psi_I^{qp}\rangle = a_{l_1}^\dagger a_{l_2}^\dagger \cdots a_{l_I}^\dagger \cdots a_{l_L}^\dagger b_{r_1}^\dagger b_{r_2}^\dagger \cdots b_{r_R}^\dagger \mid vac^{qp}\rangle \tag{3.44}$$

$$\mid \Psi_F^{qp}\rangle = a_{l}^\dagger a_{l_2}^\dagger \cdots a_{l_L}^\dagger b_{r_1}^\dagger b_{r_2}^\dagger \cdots b_{r_F}^\dagger \cdots b_{r_R}^\dagger \mid vac^{qp}\rangle \tag{3.45}$$

$$\mid \Psi_I^{ph}\rangle = c_{m_1}^\dagger c_{m_2}^\dagger \cdots c_{m_I}^\dagger \mid vac^{ph}\rangle \tag{3.46}$$

$$\mid \Psi_F^{ph}\rangle = c_{m_1'}^\dagger c_{m_2'}^\dagger \cdots c_{m_F'}^\dagger \mid vac^{ph}\rangle \tag{3.47}$$

where $\mid vac^{qp}\rangle \mid$ (resp. $\mid vac^{ph}\rangle$) denotes the quasiparticle (resp. photon) vacuum state with no particles. We have dropped the spin indices for simplicity.

Note that states $\mid \Psi_I^{qp}\rangle$ and $\mid \Psi_F^{qp}\rangle$ differ only by the occupancy of the two quasiparticle states indexed by l_I and r_F whereas $\mid \Psi_I^{ph}\rangle$ and $\mid \Psi_F^{ph}\rangle$ differ a priori by the occupancy of an arbitrary number of photon states, given the form of the exponential factor in $\widetilde{\mathcal{H}}_t$. The energy difference $E_I - E_F$ is the sum of three terms

$$E_I - E_F = \Delta\mathcal{E} + \Delta E^{qp} + \Delta E^{ph} \tag{3.48}$$

where

$$\Delta E^{qp} = \epsilon_{l_I} - \epsilon_{r_F} \tag{3.49}$$

$$\Delta E^{ph} = E_I^{ph} - E_F^{ph} = \sum_{m_i} \hbar\omega_{m_i} - \sum_{m_i'} \hbar\omega_{m_i'} \tag{3.50}$$

In the standard tunneling rate calculations, the photon degrees of freedom are absent and one finds

$$\Gamma_{I\to F} = \frac{2\pi}{\hbar} \left|t_{l_I r_F}\right|^2 \delta(\Delta\mathcal{E} + \epsilon_{l_I} - \epsilon_{r_F}) \tag{3.51}$$

One then replaces $\left|t_{l_I r_F}\right|^2$ by the average $\left|t_{av}\right|^2$ and one gets the ideal voltage bias result

$$\Gamma_j^+ \left\{Re\left[Z(\omega) = 0\right]\right\} = \frac{1}{e^2 R_t} \int dE dE' f(E) \left[1 - f(E')\right] \delta(\Delta\mathcal{E} + E - E') \tag{3.52}$$

where f is the Fermi function and R_t the tunnel resistance of the junction given by

$$R_t^{-1} = 4\pi^2 R_K^{-1} \left|t_{av}\right|^2 \rho_l\left(E_F\right) \rho_r\left(E_F\right) \tag{3.53}$$

where $\rho_l\left(E_F\right)$ (resp. $\rho_r\left(E_F\right)$) is the density of states at the Fermi level in the left (resp. right) electrode (note that, for clarity, we have dropped the junction index j in the matrix elements and in the tunnel resistance). Using the mathematical properties of the Fermi function and $\Delta\mathcal{E} \ll E_F$, the last result can be further simplified and one finally finds the well known tunnel junction formula

$$\Gamma_j^+ \left\{Re\left[Z(\omega) = 0\right]\right\} = \frac{1}{e^2 R_t} \frac{\Delta\mathcal{E}}{1 - \exp\left(-\beta_{qp}\Delta\mathcal{E}\right)} \tag{3.54}$$

where $\beta_{qp} = k_B T_{qp}$ is the inverse electronic temperature of the junction. By summing the forward and backward tunnel rates Γ_j^+ and Γ_j^- one finds that the current I through a junction directly biased by a voltage source V is given, whatever the value of β_{qp}, by $I = V/R_t$, hence the name "tunnel resistance". The independence of R_t with respect to the voltage comes from the assumption of energy independent tunnel matrix elements. More generally, one can introduce the transparency of the tunnel barrier as a function of energy:

$$\mathcal{T}(E) = 4\pi^2 \sum_{l,r} \left|t_{lr}\right|^2 \delta\left(\epsilon_l - E\right) \delta\left(\epsilon_r - E\right) \tag{3.55}$$

which is defined in such a way that $R_t = R_K \left[\mathcal{T}(E_F)\right]^{-1}$ and from which one can define the barrier traversal time [6]

$$\tau_{tr} = \hbar \frac{\partial \ln \mathcal{T}(E)}{\partial E} \tag{3.56}$$

For typical junctions $\tau_{tr} \sim 10^{-15}$s which is much shorter than any other relevant time scale in the circuit, in particular the time scales involved in the charge relaxation function $\mathcal{R}(t)$. This is why tunneling can be considered to be instantaneous in the present theory.

The inclusion of the photon degrees of freedom is a relatively straightforward extension of the calculation leading to Eq. (3.54). In addition to quasiparticle states, the sum over all initial and final states must now include the photon states. One finds

$$\Gamma_j^+ = \frac{1}{e^2 R_t} \int_{-\infty}^{+\infty} \frac{E dE}{1 - \exp(-\beta_{qp} E)} P(\Delta\mathcal{E} - E) \tag{3.57}$$

where $P(E)dE$ is the probability of an inelastic tunnel event in which the environment modes absorb a set of photons representing a total excitation energy comprised between E and $E + dE$ (more precisely, $E > 0$ corresponds to photon absorption by the environment whereas $E < 0$ corresponds to emission). The function $P(E)$ is given by

$$P(E) = \sum_{I,F} p_I^{ph} \left| \langle \Psi_F^{ph} \mid \exp(i\varphi) \mid \Psi_I^{ph} \rangle \right|^2 \delta\left(E_I^{ph} - E_F^{ph} - E\right) \tag{3.58}$$

where $\varphi = e\Phi/\hbar$ and where

$$p_I^{ph} = \langle \Psi_I^{ph} \mid \frac{\exp\left(-\beta \widetilde{\mathcal{H}}'_{\mathrm{E}}\right)}{\mathrm{tr}\left[\exp\left(-\beta \widetilde{\mathcal{H}}'_{\mathrm{E}}\right)\right]} \mid \Psi_I^{ph} \rangle \tag{3.59}$$

We have introduced in the last equation the inverse temperature β of the environment which is not necessarily equal to the junction electron inverse temperature β_{qp}. Using the Fourier transform of the δ function and noting $\langle \cdots \rangle_{\mathrm{E}}$ an environment average involving β we obtain

$$P(E) = \frac{1}{2\pi\hbar} \int_{-\infty}^{+\infty} dt \mathrm{e}^{\frac{i}{\hbar} Et} \langle \mathrm{e}^{i\varphi(t)} \mathrm{e}^{-i\varphi(0)} \rangle_{\mathrm{E}} \tag{3.60}$$

By definition $\varphi(t) = \mathrm{e}^{i\widetilde{\mathcal{H}}'_{\mathrm{E}} t} \varphi \mathrm{e}^{-i\widetilde{\mathcal{H}}'_{\mathrm{E}} t}$ and thus $[\varphi(t), \varphi(0)] \neq 0$. However, since φ is a linear combination of creation and anihilation operators for harmonic oscillator modes, we have

$$\langle \mathrm{e}^{i\varphi(t)} \mathrm{e}^{-i\varphi(0)} \rangle_{\mathrm{E}} = \mathrm{e}^{-\langle [\varphi(t) - \varphi(0)] \varphi(0) \rangle_{\mathrm{E}}} \tag{3.61}$$

The flux–flux correlation function can be expressed in terms of $\mathrm{Re}\left[Z_{\mathrm{E}}(\omega)\right]$ by the quantum fluctuation–dissipation theorem [61]:

$$S_\Phi(\omega) = \frac{\hbar^2}{e^2}\int_{-\infty}^{+\infty} dt e^{i\omega t}\left\langle\varphi(t)\varphi(0)\right\rangle_{\mathrm{E}} \tag{3.62}$$

$$= \frac{1}{\omega^2}\frac{2\hbar\omega}{1-\mathrm{e}^{-\beta\hbar\omega}}\mathrm{Re}\left[Z_{\mathrm{E}}(\omega)\right] \tag{3.63}$$

In the classical limit $\beta\hbar\omega \to 0$, one recovers the usual fluctuation–dissipation theorem: the voltage–voltage correlation function of the environment, which is the second derivative of $\left\langle\Phi(t)\Phi(0)\right\rangle_{\mathrm{E}}$, is given by the product $k_{\mathrm{B}}T\mathcal{R}(t)$ of the environment temperature and the charge relaxation function.

Using the identity $2\left(1-\mathrm{e}^{-\beta\hbar\omega}\right)^{-1} = 1+\coth\left(\frac{1}{2}\beta\hbar\omega\right)$ and the symmetry of $\mathrm{Re}\left[Z_{\mathrm{E}}(\omega)\right]$ we arrive finally at

$$P(E) = \frac{1}{2\pi\hbar}\int_{-\infty}^{+\infty} dt \exp\left[\frac{i}{\hbar}Et + J(t)\right] \tag{3.64}$$

with

$$J(t) = 2\int_0^{+\infty}\frac{d\omega}{\omega}\frac{\mathrm{Re}\left[Z_{\mathrm{E}}(\omega)\right]}{R_K}\left\{\coth\left(\frac{1}{2}\beta\hbar\omega\right)\left[\cos(\omega t)-1\right] - i\sin(\omega t)\right\} \tag{3.65}$$

Expressions (3.57), (3.64) and (3.65) display the precise mathematical relationship between the tunneling rate in presence of an arbitrary environment and the impedance of that environment, as well as the role of the energy difference $\Delta\mathcal{E}$.

3.7. Properties of $P(E)$

From Eqs. (3.64) and (3.65) we can establish the general properties of the probability function $P(E)$:

$$\int_{-\infty}^{+\infty} P(E)dE = 1 \tag{3.66}$$

$$\int_{-\infty}^{+\infty} P(E)EdE = \frac{e^2}{2}\mathcal{R}(t=0) = \frac{e^2}{2}\left(C_j^{-1} - C_0^{-1}\right) \tag{3.67}$$

$$P(-E) = \exp\left(-\beta E\right)P(E) \tag{3.68}$$

It is possible to show quite generally from the form of $J(t)$ that, in the low impedance environment limit defined by $\frac{1}{R_K}\int_0^{+\infty}\mathcal{R}(t)dt \to 0$, the function $P(E)$ tends towards $\delta(E)$. In the high impedance limit defined by $\frac{1}{R_K}\int_0^{+\infty}\mathcal{R}(t)dt \to \infty$, the function $P(E)$ tends towards $\delta\left[E - \frac{e^2}{2}\mathcal{R}(t=0)\right]$, provided that $k_BT \ll$

$\frac{e^2}{2}\mathcal{R}(t=0)$. These limits correspond to the application range of the so-called "global rules" and "local rules" [62]. According to these rules, the tunneling rate involves only the change in either the global energy of the whole circuit (the energy we have labeled $\mathcal{E}$) or the local electrostatic energy of the sole junction.

In practise, there is a considerable bias in favor of the global rules: without any particular engineering effort the charge relaxation integral $\int_0^{+\infty}\mathcal{R}(t)dt$ tends to be of the order of the impedance of the vacuum $Z_{\rm vac}\simeq 377\Omega$. It is worth noting that there is a fundamental relation between the impedance of the vacuum and the resistance quantum: $Z_{\rm vac}=2\alpha R_K$ where $\alpha=1/137.0\ldots$ is the fine structure constant. We thus live in a world where it is difficult to escape from the global rules!

We will now consider three useful examples of the environment impedance $Z_e(\omega)$.

3.8. *Application of the theory to particular cases of junction environments*

3.8.1. *Ohmic case*

This case corresponds to a junction in series with a frequency independent resistance $Z_e(\omega)=R$ and a voltage source V. We have $C_0^{-1}=0$ and the energy difference $\Delta\mathcal{E}$ is given simply by $\Delta\mathcal{E}=eV$. At $T=0$ we find that the function $P(E)$ is non analytic at $E=0$ and that there is a divergence given by

$$P(E)=\frac{\exp(-\gamma/g)}{\Gamma(g)}\frac{1}{E}\left|\frac{2\pi}{g}\frac{E}{E_c}\right|^{1/g}+\mathcal{O}(E^{1/g}) \tag{3.69}$$

where γ is the Euler constant, $\Gamma(x)$ the gamma function, $E_c=e^2/2C_j$ and g the dimensionless conductance $g=\frac{1}{2}R_K/R$. Note that when $g\gg 1$ (low impedance limit) the form of $P(E)$ tends towards that of a δ function.

The divergence at $E=0$ implies that the differential conductance dI/dV should go to zero at small voltages $V\ll e/C_j$ and low temperatures $k_BT, k_BT_{qp}\ll E_c$:

$$dI/dV \underset{\substack{V\to 0\\ T\to 0}}{\sim} |V|^{1/g} \tag{3.70}$$

A convincing observation of this zero-bias anomaly has been performed by Cleland et al. [25] who have placed thin film resistors close to the junction.

3.8.2. *Case of an electron box with a non ideal voltage bias*

In this case the junction is in series with a capacitor C_s, a resistor R and a voltage source U. The environment impedances are $Z_e(\omega)=R+i/C_s\omega$ and $Z_{\rm E}=(1+iRC_s\omega)/\left(iC_\Sigma\omega-RC_jC_s\omega^2\right)$ where $C_\Sigma=C_j+C_s$. The

series capacitance C_0 is equal to the total capacitance C_Σ of the island and $\Delta\mathcal{E} = e\left[C_s U - (n+1/2)\,e\right]/C_\Sigma$. One finds the same divergence at $T = 0$ for $P(E)$ when $E \to 0$ as in Eq. (3.69), but now the exponent g is given by $g = \frac{1}{2}R_K/\mathrm{Re}\left[Z_\mathrm{E}(0)\right] = \frac{1}{2}C_\Sigma R_K/\left(RC_s\right)$ [62]. Since in the electron box experiments $R \sim 0.01R_K$ and $C_s \sim 0.05C_\Sigma$ this analysis shows that the global rule $P(E) = \delta(E)$ is an excellent approximation in this case. We can also apply the same analysis to junction array circuits like the SET transistor or the pump for which one must take $C_s \sim C_\Sigma/\mathtt{N}$ where $\mathtt{N}$ is the number of junctions in the array. Again we find that the global rules are very good for usual voltage sources and become exact in the limit $\mathtt{N} \to \infty$.

3.8.3. Single mode case

In this case the junction is in series with a pure inductor ($Z_e(\omega) = iL\omega$) and a voltage souce V. The a.c. environment of the tunnel element thus consists of a single mode whose frequency is given $\omega_1 = (LC_j)^{-1/2}$. We find that $J(t)$ is an oscillatory function and this in turn implies that the function $P(E)$ reduces to a series of δ functions

$$P(E) = \sum_{\mathsf{N}} \frac{r^{\mathsf{N}}}{\mathsf{N}!} \exp(-r)\,\delta\left(E + \mathsf{N}\hbar\omega_1 - eV\right) \tag{3.71}$$

where the parameter r measures the ratio between the Coulomb energy $e^2/2C_j$ and the energy level separation of the oscillator.

$$r = \frac{e^2/2C_j}{\hbar\omega_1} = \pi\frac{\sqrt{L/C_j}}{R_K} \tag{3.72}$$

The differential conductance dI/dV displays steps at $V = \mathsf{N}\frac{\hbar}{e}\omega_1$. These steps have been observed by Holst et al. [63] in an experiment where the junction was coupled to a voltage source via a transmission line resonator which played the role of an inductor.

We clearly see in this single mode case the effect of the quantization of the environment modes. In the extreme quantum limit $r \ll 1$, corresponding to an oscillator with an impedance small compared with the resistance quantum, the function $P(E)$ essentially consists of an elastic peak at $E = 0$. On the other hand, in the classical limit $r \gg 1$, the enveloppe of the peaks takes the shape of a gaussian function centered at $E = e^2/2C_j$.

Let us consider the tunnel process associated with the $\mathsf{N} = 0$ elastic channel. The rate of this process is finite since the excitation energy of the oscillator is quantized. This process is the only one allowed when $eV < \hbar\omega_1$. In this case the voltage generates directly an electron–hole pair in the junction without exciting the oscillator, which in classical term would mean without charging the capacitor.

Table 2

Correspondence between elastic tunneling and the Mössbauer effect.

Junction	γ-Ray emitter
Capacitance C	Mass of atom
Inductance L	Effective spring constant
Voltage V	γ-Ray energy in atom frame
2nd derivative of $I(V)$ curve	γ-Ray spectrum in lab frame
Tunneling without charging	Emission without recoil
Charge comes directly from source	Crystal takes all recoil momentum

This may seem paradoxical since the source is usually much farther than the junction "electromagnetic horizon" $c\tau_{tr}$ where c is the speed of light. The resolution of this paradox lies in the non-local character of quantum mechanics. The junction and the source are in a coherent quantum state. When this state changes, both the source and junction are affected at the same time. Instantaneous transmission of information is impossible, though: in the conditions under which tunneling without charging occurs, the charge fluctuations on the junction capacitance are much larger than e. The source is therefore not able to "notice" the occurence of a tunnel event.

Fully elastic tunneling or equivalently, tunneling without charging, is analogous to γ-ray emission without recoil in the Mössbauer effect. A γ-ray emitter such as a ^{60}Co nucleus in a cristal of ^{59}Co can be thought of as being elastically bound to the rest of the crystal. The equivalence between the γ-ray emitter and the junction is given in Table 2.

4. Single Cooper pairs

As we have seen in the first part of this course, the theory developed for normal metal tunnel junction circuits can be extended to superconducting ones. Superconductivity introduces new energy scales: the superconducting gap energy Δ, the even-odd free energy $\widetilde{D}(T)$ and the Josephson energy E_J. In this last part of the course, we will concentrate on the theory of the even-odd free energy $\widetilde{D}(T)$ which is a unique feature of mesoscopic superconducting systems revealed by charging effects. Before examining how Coulomb charging effects can interplay with superconductivity and lead to the observation of single Cooper pair transfer, we will review first the theory of superconductivity by Bardeen, Cooper and Schrieffer (BCS) [64], which up to now has proven entirely satisfactory in the field of single charge phenomena.

4.1. Basic elements of the BCS theory

The BCS theory starts by assuming that the metal which undergoes a superconducting transition can be treated in the normal state by Fermi-liquid theory, namely that its excitations not far above the Fermi ground state are described by fermionic quasiparticles. It is convenient to introduce the set of eigenfunctions $\Psi_\kappa(\mathbf{x}, \sigma)$ of the quasiparticle kinetic energy operator. Here $\mathbf{x}$ and σ denote the position and spin of the quasiparticle, respectively. In the case of perfect translational symmetry, the Ψ's are plane waves and the index κ corresponds to the wavenumber. The theory can also handle the case of a "dirty" metal, i.e. a realistic metal with impurities and walls, for which the Ψ's are unknown functions whose main statistical properties are known nevertheless. In this latter case the index κ is a label with no special meaning. In presence of time-reversal symmetry, to each state $\mid k\rangle$ which we define as corresponding to the wavefunction $\Psi_\kappa(\mathbf{x}, \uparrow)$, we can associate a time-reversed mate state $\mid \overline{k}\rangle$ corresponding to the wavefunction $\Psi^*_\kappa(\mathbf{x}, \downarrow)$ and having the same energy. The couples $K = \{\mid k\rangle, \mid \overline{k}\rangle\}$ are the basic objects of BCS theory.

The next step in BCS theory is to assume that the metal is described by the many-body hamiltonian

$$\mathcal{H} = \sum_{K \in \mathcal{C}} (\epsilon_K - E_\mathrm{F}) \left(a^\dagger_k a_k + a^\dagger_{\overline{k}} a_{\overline{k}} \right) + \sum_{K,L \in \mathcal{C}} V_{KL} a^\dagger_k a^\dagger_{\overline{k}} a_{\overline{l}} a_l \tag{4.1}$$

where the a's are the quasiparticle annihilation operators corresponding to the Ψ's, the ϵ's the kinetic energies of the quasiparticles and the V's the matrix elements of the quasiparticle–quasiparticle interaction. The symbol E_F denotes the energy of the Fermi level while the sums $\sum_{K \in \mathcal{C}}$ and $\sum_{K,L \in \mathcal{C}}$ extend in a neighbourhood $\mathcal{C}$ of the Fermi level where quasiparticle levels are well defined. The neighbourhood $\mathcal{C}$ is such that its width in energy is small compared with the Fermi energy while being sufficiently large to encompass the Debye energy which fixes the range of the interaction.

One then introduces the pairing amplitude $A_K = \langle a_{\overline{k}} a_k \rangle$ and the pair potential $\Delta_K = -\sum_L V_{KL} A_L$. Next, a crucial step is taken by assuming that one can neglect the fluctuations $a_{\overline{k}} a_k - A_K$ (mean field approximation). With this hypothesis, the diagonalization of the hamiltonian (4.1) becomes equivalent to the diagonalization of the self-consistent mean field hamiltonian

$$\mathcal{H}_M = \sum_{K \in \mathcal{C}} \left[(\epsilon_K - E_\mathrm{F}) \left(a^\dagger_k a_k + a^\dagger_{\overline{k}} a_{\overline{k}} \right) - \Delta_K a^\dagger_k a^\dagger_{\overline{k}} - \Delta^*_K a_k a_{\overline{k}} + \Delta_K A^*_K \right] \tag{4.2}$$

Obviously, an eigenfunction of $\mathcal{H}_M$ is of the form $\prod_K \chi_K \mid \mathrm{vac}\rangle$ where χ_K is a second quantization operator in the manifold K and $\mid \mathrm{vac}\rangle$ the quasiparticle

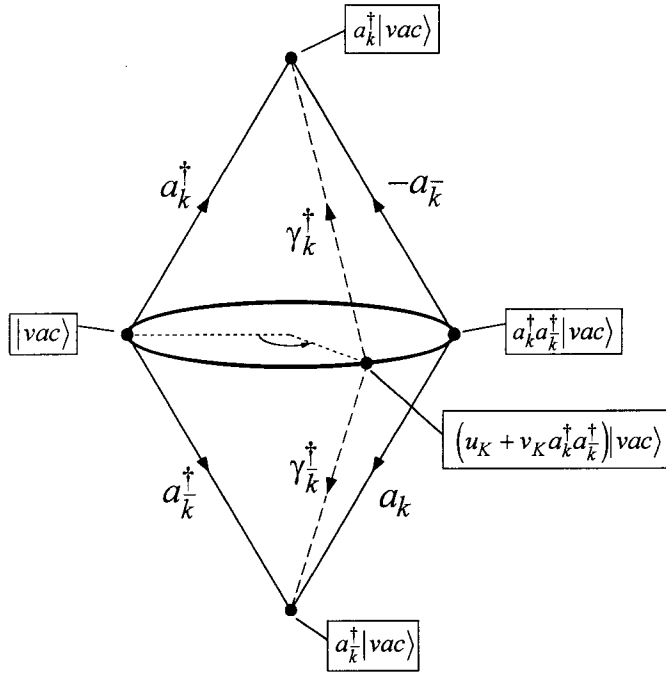

Fig. 13. Graphical representation of the Bogoliubov–Valatin transformation in the manifold $K = \{k, \bar{k}\}$

vacuum state. In order for the product $\prod_K \chi_K$ to have a value independent of the order of the operators (apart from an overall phase factor), the only allowed possibilities for the operator χ_K are either $a_k^\dagger$, $a_{\bar{k}}^\dagger$ or the linear combination $u_K + v_K a_k^\dagger a_{\bar{k}}^\dagger$ where u_K and v_K are two arbitrary complex numbers such that $|u_K|^2 + |v_K|^2 = 1$. Note that $\lambda_K a_k^\dagger + \mu_K a_{\bar{k}}^\dagger$, for example, does not qualify as a meaningful χ_K.

The transformation which transforms $|\text{ vac}\rangle$ into $\left(u_K + v_K a_k^\dagger a_{\bar{k}}^\dagger\right) |\text{ vac}\rangle$ in state vector space induces the transformation of $a_k^\dagger$ and $a_{\bar{k}}^\dagger$ into

$$\gamma_k^\dagger = u_K a_k^\dagger - v_K a_{\bar{k}} \tag{4.3}$$

$$\gamma_{\bar{k}}^\dagger = u_K a_{\bar{k}}^\dagger + v_K a_k \tag{4.4}$$

as shown graphically on Fig. 13.

A transformation specified by expressions (4.3) and (4.4) is called a Bogoliubov–Valatin transformation.

The Fermi-liquid many-body ground state, i.e. the ground state of

$$\mathcal{H}_{FL} = \sum_{K \in \mathcal{C}} (\epsilon_K - E_{\rm F}) \left(a_k^\dagger a_k + a_{\bar{k}}^\dagger a_{\bar{k}} \right), \tag{4.5}$$

is $\mid \mathrm{G_{Fermi}} \rangle = \prod_{K \in \mathcal{C}} \left(u_K^{\rm F} + v_K^{\rm F} a_k^\dagger a_{\bar{k}}^\dagger \right) \mid \mathrm{vac} \rangle$ with $u_K^{\rm F} = \Theta(\epsilon_K - E_{\rm F})$ and $v_K^{\rm F} = \Theta(E_{\rm F} - \epsilon_K)$, $\Theta(x)$ being the Heaviside function.

The ground state of the hamiltonian (4.2), the so-called BCS ground state, is also of the form

$$\mid \mathrm{G_{BCS}} \rangle = \prod_{K \in \mathcal{C}} \left(u_K + v_K a_k^\dagger a_{\bar{k}}^\dagger \right) \mid \mathrm{vac} \rangle \tag{4.6}$$

but with

$$u_K v_K^* = \frac{\Delta_K}{2\sqrt{|\Delta_K|^2 + (\epsilon_K - E_{\rm F})^2}} \tag{4.7}$$

This last equation determines u_K and v_K (apart from an overall phase factor which is irrelevant) since Δ_K is determined by the condition for self-consistency

$$\Delta_K = -\frac{1}{2} \sum_L \frac{\Delta_L}{\sqrt{|\Delta_K|^2 + (\epsilon_K - E_{\rm F})^2}} V_{KL} \tag{4.8}$$

Note that $u_K^{\rm F}, v_K^{\rm F}$ is a trivial solution of (4.7) and (4.8) with $\Delta_K = 0$. However, when $V_{KL} < 0$, Eq. 4.8 admits a non-trivial solution such that $\Delta_K \neq 0$ and whose energy is lower than for $u_K^{\rm F}, v_K^{\rm F}$. In the model of BCS where

$$V_{KL} = \begin{cases} -V & \text{if} \quad |\epsilon_K - E_{\rm F}| \leq \hbar\omega_c \quad \text{and} \quad |\epsilon_L - E_{\rm F}| \leq \hbar\omega_c \\ 0 & \text{otherwise} \end{cases} \tag{4.9}$$

one finds

$$\Delta_K = \begin{cases} \Delta & \text{for} \quad |\epsilon_K - E_{\rm F}| < \hbar\omega_c \\ 0 & \text{for} \quad |\epsilon_K - E_{\rm F}| > \hbar\omega_c \end{cases} \tag{4.10}$$

where V is a positive constant and ω_c a cut-off frequency set by the Debye energy. In this model the energy-independent parameter Δ is given by

$$\Delta = \frac{\hbar\omega_c}{\sinh\left[\rho_{\rm F} V\right]} \exp\left(i\theta\right) \tag{4.11}$$

where $\rho_{\rm F}$ is the density of states at the Fermi level and $\exp\left(i\theta\right)$ an arbitrary phase factor. The values of u_K and v_K are then determined easily:

$$u_K = \sin\left[\frac{1}{2}\arctan\left(-\frac{|\Delta|}{\epsilon_K - E_F}\right)\right] \tag{4.12}$$

$$v_K = \sqrt{1 - u_K^2}\exp(i\theta) \tag{4.13}$$

With the preceding expressions one can calculate the condensation energy

$$\delta U = \langle G_{BCS} \mid \mathcal{H}_M \mid G_{BCS}\rangle - \langle G_{Fermi} \mid \mathcal{H}_M \mid G_{Fermi}\rangle \tag{4.14}$$

and find

$$\delta U = -\frac{1}{2}\rho_F \Delta^2 = -\frac{1}{2}\mathcal{P}\Delta \tag{4.15}$$

The quantity $\mathcal{P}$ is often called the number of Cooper pairs in the system: it is the number of manifolds K such that the product $|u_K v_K|$ is of order unity, i.e. manifolds for which the state occupancy differs notably from the corresponding occupancy in $\mid G_{Fermi}\rangle$. In the weak coupling limit $\rho_F V \ll 1$ which describes the case of aluminium — the superconductor on which our experiments are based — we have $\mathcal{P} \ll \mathcal{N}$, where $\mathcal{N}$ denotes the total number of electrons.

Note that the average condensation energy per electron is $\frac{1}{2}\mathcal{P}\Delta/\mathcal{N} \sim \Delta^2/E_F$ where $\Delta/E_F \sim 10^{-4}$. Adding two electrons to the system increases therefore the condensation energy by a negligible amount compared with Δ. As we are now going to see, adding *one* electron is a totally different matter.

Due to the particular properties of the χ_K operator space, the coefficients u_K and v_K corresponding to the ground state [Eq. (4.6)] are precisely those corresponding to the Bogoliubov–Valatin transformation which diagonalizes the mean-field hamiltonian (4.2) (In general, the components of the ground state vector in a Hilbert space do not suffice to determine the transformation which makes the hamiltonian a diagonal operator). The mean-field hamiltonian thus takes the form

$$\mathcal{H}_M = \sum_{K\in\mathcal{C}} E_K\left(\gamma_k^\dagger\gamma_k + \gamma_{\bar{k}}^\dagger\gamma_{\bar{k}}\right) + \delta U \tag{4.16}$$

where

$$E_K = \sqrt{|\Delta_K|^2 + (\epsilon_K - E_F)^2} \tag{4.17}$$

determines the excitation spectrum. In the model given by (4.9) this spectrum has a gap given by Δ, hence the name often given to this quantity.

It is interesting to note that while the ground state obeys

$$\gamma_k \mid G_{BCS}\rangle = \gamma_{\bar{k}} \mid G_{BCS}\rangle = 0 \tag{4.18}$$

an excited state with a single excitation is such that

$$\gamma_k^\dagger \mid \mathrm{G_{BCS}}\rangle = a_k^\dagger \prod_{\substack{L\in\mathcal{C}\\ L\neq K}} \left(u_L + v_L a_l^\dagger a_{\bar{l}}^\dagger\right) \mid \mathrm{vac}\rangle \tag{4.19}$$

or

$$\gamma_{\bar{k}}^\dagger \mid \mathrm{G_{BCS}}\rangle = a_{\bar{k}}^\dagger \prod_{\substack{L\in\mathcal{C}\\ L\neq K}} \left(u_L + v_L a_l^\dagger a_{\bar{l}}^\dagger\right) \mid \mathrm{vac}\rangle \tag{4.20}$$

Thus, a single particle excitation of the superconductor has just the same wavefunction as an ordinary excitation of the normal state. We need the operator $\gamma_k^\dagger$ to produce it from $\mid \mathrm{G_{BCS}}\rangle$ — and not $a_k^\dagger$ — since the latter does not produce a state othogonal to $\mid \mathrm{G_{BCS}}\rangle$. Adding one electron to a superconductor with all electrons paired must therefore decrease by Δ the magnitude of the condensation energy. In order for this change to be observable, the superconductor has to be isolated from a particle reservoir.

4.2. Extension of the BCS theory to an isolated superconductor

We have now to face the problem that while the BCS hamiltonian (4.1) conserves the total number of particles, the mean-field hamiltonian (4.2) does not. This is why the BCS wavefunction (4.6) turns out to be a linear superposition of states with different number of particles. This symmetry breaking in Fock space is completely unphysical if the superconductor is isolated from a particle reservoir. A remedy found by Anderson [65] is first to note that there is not one BCS ground state but many since all the states

$$\mid \mathrm{G}_{\mathrm{BCS}}^\theta\rangle = \prod_{K\in\mathcal{C}} \left(|u_K| + |v_K| \exp(i\theta)\, a_k^\dagger a_{\bar{k}}^\dagger\right) \mid \mathrm{vac}\rangle \tag{4.21}$$

correspond to different linear combinations of states with a well-defined particle number, even if they have the same energy according to (4.2). We can then form

$$\mid \mathrm{G}_{\mathrm{A}}^P\rangle = \frac{1}{2\pi}\int_0^{2\pi} d\theta \exp(-iP\theta) \mid \mathrm{G}_{\mathrm{BCS}}^\theta\rangle \tag{4.22}$$

This linear superposition of BCS ground states projects out of $|\mathrm{G}_{\mathrm{BCS}}^{\theta=0}\rangle$ the part that has P pairs of particles occupying the levels of $\mathcal{C}$. Numerical studies [66] have shown that the state given by Eq. (4.22) is very close energetically to the true non-degenerate ground state of the full BCS hamiltonian (4.1) for an isolated system with an even number $N = 2P$ of particles, as soon as N gets large.

What about the ground state of an isolated system with an odd number $N = 2P + 1$ of particles? One state of a manifold K has then to be occupied with certainty by an unpaired electron. Using the method of Eq. (4.22) we can fulfill this condition with the two following states

$$| \, \mathrm{G}_{\mathrm{A}}^{P+\frac{1}{2}} \rangle = \gamma_{\kappa}^{\dagger} \, | \, \mathrm{G}_{\mathrm{A}}^{P} \rangle \tag{4.23}$$

where $\kappa = k_{\mathrm{F}}$ or $\overline{k}_{\mathrm{F}}$. The expression of the odd ground state given by (4.23) is

$$| \, \mathrm{G}_{\mathrm{A}}^{P+\frac{1}{2}} \rangle = \int_0^{2\pi} d\theta \exp\left(-iP\theta\right) a_{\kappa}^{\dagger} \prod_{L \neq K} \left(|u_L| + |v_L| \exp\left(i\theta\right) a_l^{\dagger} a_{\overline{l}}^{\dagger} \right) | \, \mathrm{vac} \rangle \tag{4.24}$$

The numerical studies cited above have confirmed that this type of linear combination also describes the degenerate ground states of the odd-N isolated system quite well.

4.3. Partition function of the superconducting electron box

We now consider a box in which only the island is superconducting. The electron reservoir to which the island is connected by a tunnel junction remains in the normal state. We assume that the internal energy of the island of the electron box is well described by the hamiltonian of Eq. (4.1). Now E_{F} refers to the energy of the Fermi level when the island is neutral (for an island reduced to a molecule, E_{F} would be the average between the HOMO and LUMO energy). In order to form the hamiltonian of the box, we now need to express the electrostatic energy in terms of the quasiparticle degrees of freedom. Although we do not know exactly the total number $\mathcal{N}_0$ of electrons in the island when it is neutral nor the number $N_0 = \sum_{K \in \mathcal{C}} \Theta(E_{\mathrm{F}} - \epsilon_K)$ of quasiparticles in the domain $\mathcal{C}$ lying below E_{F} in the ground state, the operator associated with the number of excess electrons is well-defined:

$$n = \mathcal{N} - \mathcal{N}_0 = \sum_{K \in \mathcal{C}} \left(a_k^{\dagger} a_k + a_{\overline{k}}^{\dagger} a_{\overline{k}} \right) - N_0 \tag{4.25}$$

The previous relation is a consequence of the fundamental property of Fermi-liquid theory that there is precisely one quasiparticle which is created for every bare electron which is added to the system [67].

If one introduces the charge imbalance operator [68]

$$\mathcal{Q} = \sum_{K \in \mathcal{C}} \left(|u_K|^2 - |v_K|^2 \right) \left(\gamma_k^{\dagger} \gamma_k + \gamma_{\overline{k}}^{\dagger} \gamma_{\overline{k}} \right) \tag{4.26}$$

the constraint expressed in Eq. (4.25) becomes equivalent to:

$$\langle n, k_1, k_2, \ldots k_M \mid \mathcal{Q} \mid n, k_1, k_2, \ldots k_M \rangle = 0 \tag{4.27}$$

where $\mid n, k_1, k_2, \ldots k_M \rangle$ is a state of the island analogous to (4.24) but with n excess electrons and quasiparticle excitations in levels k_1, k_2,... k_M (this state is a function of the numbers v_k).

If we assume that mean field theory applies to the island, the hamiltonian of the electron box can therefore be written

$$\mathcal{H} = \sum_{K \in \mathcal{C}} E_K \left(\gamma_k^\dagger \gamma_k + \gamma_{\bar{k}}^\dagger \gamma_{\bar{k}} \right) + E_C \left(n - n_x \right)^2 + \mathcal{H}_T \tag{4.28}$$

Here $\mathcal{H}_T$ is the tunnel hamiltonian describing the exchange of electrons between the island and the reservoir and $n_x = C_s U/e$ the externally varied offset charge. The island is sufficiently large that E_K is given by Eq. (4.17) with a n-independent E_F. We have not included in the right-hand side of Eq. (4.28) n-independent terms or terms only weakly dependent on n such as δU.

Let us now introduce the number of quasiparticle excitations

$$N_{qp} = \sum_{K \in \mathcal{C}} \left(\gamma_k^\dagger \gamma_k + \gamma_{\bar{k}}^\dagger \gamma_{\bar{k}} \right) \tag{4.29}$$

The operators N_{qp} and n are not independent. For island states which have a well defined number of electrons such as $\mid n, k_1, k_2, \ldots k_M \rangle$, one can show that the parity of N_{qp} must be equal to the parity of the total number of electrons. Thus

$$\left[\langle N_{qp} \rangle - \mathcal{N}_0 \right] \bmod 2 = \langle n \rangle \bmod 2 \tag{4.30}$$

It is important to realize that this new constraint is totally independent from the constraint expressed by Eq. (4.27): for example quasiparticle levels lying above and below the Fermi level contribute identically to Eq. (4.30) whereas they contribute with opposite signs to Eq. (4.27).

We now compute $Z = \mathrm{tr} \exp\left(-\beta \mathcal{H}\right)$ where $\beta = \left(k_\mathrm{B} T\right)^{-1}$ and where the trace is taken over all states with a given number of excess electrons.

$$Z = \sum_n Z_n^{qp} \exp\left[-\beta E_C \left(n - n_x \right)^2 \right] \tag{4.31}$$

In this expression we have neglected the effect of the tunneling hamiltonian which is treated as a weak perturbation. If we did not have the constraints Eq. (4.27) and Eq. (4.30) Z_n^{qp} would be given by

$$Z_+^{qp} = \prod_{K \in \mathcal{C}} \left[1 + \exp\left(-\beta E_K \right) \right]^2 \tag{4.32}$$

the usual partition function for free fermions in a system with time-reversal symmetry. It can be shown that taking into account the constraint Eq. (4.27), which is difficult analytically, will only produce small corrections which can be ignored in the large $\mathcal{N}$ limit. As shown by Jankó et al. [69], the n-dependence of the condensation energy and of the quasiparticle–quasiparticle interaction will also produce small corrections. The constraint Eq. (4.30) remains crucial even in the large $\mathcal{N}$ limit but can be taken into account analytically by the following elegant method [53]. Let us introduce

$$Z_{-}^{qp} = \prod_{K \in \mathcal{C}} \left[1 - \exp\left(-\beta E_K\right)\right]^2 \tag{4.33}$$

It is easy to show that the expression for Z_n^{qp} which takes into account the constraint (4.30) is

$$Z_n^{qp} = \frac{1}{2}\left[Z_{+}^{qp} - (-1)^n Z_{-}^{qp}\right] \tag{4.34}$$

This trick ensures that if n is even (resp. odd) only the even (resp. odd) n terms are kept in Z_{+}^{qp}.

If we now define the odd-even free energy difference $\widetilde{D}(\beta)$ by

$$\exp\left(-\beta\widetilde{D}\right) = \frac{Z_1^{qp}}{Z_0^{qp}} = \frac{\left[Z_{+}^{qp} - Z_{-}^{qp}\right]}{\left[Z_{+}^{qp} + Z_{-}^{qp}\right]} \tag{4.35}$$

we finally arrive at

$$Z = Z_0^{qp} \sum_n \exp\left\{-\beta\left[E_C\left(n - n_x\right)^2 + p_n\widetilde{D}\right]\right\} \tag{4.36}$$

where $p_n = \frac{1}{2}\left[1 - (-1)^n\right]$.

This expression shows that in the graphical determination of the average number $\langle n \rangle$ of electrons in the superconducting box (see Fig. 9) we must indeed shift the odd-n parabolas with respect to the even-n parabolas by an amount $\widetilde{D}$.

We can express the odd-even free energy difference in terms of the density of states $\rho(\varepsilon)$ for the superconducting island. Transforming $\prod_{K \in \mathcal{C}}$ into an integral, we get

$$Z_{\pm} = \exp\left[\int_0^{+\infty} d\varepsilon \rho(\varepsilon) \ln\left(1 \pm \mathrm{e}^{-\beta\varepsilon}\right)\right] \tag{4.37}$$

from which it is easy to obtain

$$\widetilde{D}(\beta, \rho) = -\frac{1}{\beta} \ln\left(\tanh\left\{\int_0^{+\infty} \frac{d\varepsilon}{2} \rho(\varepsilon) \ln\left[\coth\left(\beta\varepsilon/2\right)\right]\right\}\right) \tag{4.38}$$

For a superconductor described by the BCS model [Eqs. (4.12) and (4.13)] the density of states is given by

$$\rho(\varepsilon) = 2\rho_A \mathcal{N}_A \mathrm{Re}\left[\frac{\varepsilon}{\sqrt{\varepsilon^2 - \Delta^2}}\right] \tag{4.39}$$

where ρ_A is the density of states per atom and $\mathcal{N}_A$ the number of atoms in the island. For temperatures $\mathrm{e}^{-\beta\Delta} \ll 1$, one finds

$$\tanh\left\{\int_0^{+\infty} \frac{d\varepsilon}{2}\rho(\varepsilon)\ln\left[\coth\left(\beta\varepsilon/2\right)\right]\right\} \approx N_{eff}\left(\beta\right)\mathrm{e}^{-\beta\Delta} \tag{4.40}$$

with

$$N_{eff}\left(\beta\right) = \mathcal{P}\left(\frac{2\pi}{\beta\Delta}\right)^{1/2} + \mathcal{O}\left[\left(\frac{1}{\beta\Delta}\right)^{3/2}\right] \tag{4.41}$$

where $\mathcal{P} = \rho_A \mathcal{N}_A \Delta$.

At temperatures such that $N_{eff}\mathrm{e}^{-\beta\Delta} \ll 1$, we get

$$\widetilde{D}(T) \simeq \Delta - k_B T \ln \mathcal{P} \tag{4.42}$$

More generally, if there are inside the gap discrete quasiparticle states with energies ϵ_i and degeneracies G_i they will strongly reduce $\widetilde{D}(T)$ which will be given in the low temperature limit by

$$\widetilde{D}(T) \simeq \epsilon_0 - k_B T \ln G_0 \tag{4.43}$$

where the index $i = 0$ refers to the lowest discrete state. Experimentally it seems possible to exclude the presence of such states in certain samples, as shown by the results presented in the first part of the course.

In the presence of a magnetic field H, the density of states given by (4.39) is no longer valid. For our "small" mesoscopic islands we can nevertheless compute the density of states within the mean field approximation, provided that the elastic mean free path is small compared to the dimension of the samples [70], which is the case in our experiments. Here "small" means that the dimensions normal to the applied magnetic field are sufficiently smaller than the London penetration length and that screening currents can be neglected. The experimental results found for $\widetilde{D}(T, H)$ are in excellent agreement with the theoretical predictions [71].

Note added in proof

We would like to emphasize that this course is not an exhaustive account of single electron phenomena, nor is the list of references by any means complete and up-to-date. Among important developments which have taken place since this course

was given is the observation of single energy levels in a nanometer-size metallic particle by Ralph et al. (Phys. Rev. Lett. **74** (1995) 3241). We hope nevertheless that we have listed enough references to enable interested readers to find their way in the literature.

Acknowledgements

We thank P. Joyez, P. Lafarge, P.F. Orfila and H. Pothier, with whom the experimental results described in this article have been obtained, for discussions and help with the figures. We are also indebted to B. Jankó for pointing out a few problems in the original manuscript. One of us (M.H.D.) is particularly grateful to the les Houches participants for stimulating questions and remarks during the oral presentation of this course. This work has been partly supported by the Bureau National de la Métrologie.

References

[1] D.M. Eigler and E.K. Schweizer, Nature **344** (1990) 524.
[2] D.J. Wineland, W.M. Itano and R.S. Van Dyck Jr., Adv. At. Mol. Phys. **19** (1983) 135.
[3] R.S. Van Dyck Jr., P.B. Schwinberg and H.G. Dehmelt, Phys. Rev. D **34** (1986) 722.
[4] R.A. Millikan, Phys. Rev. **32** (1911) 349.
[5] L. Solymar, Superconductive Tunneling (Chapman and Hall, London, 1972) Chapter 2.
[6] M. Büttiker and R. Landauer, Phys. Rev. Lett. **49** (1982) 1739.
[7] B.N.J. Personn and A. Baratoff, Phys. Rev. B **38** (1988) 9616.
[8] P. Lafarge, H. Pothier, E.R. Williams, D. Esteve, C. Urbina and M.H. Devoret, Z. Phys. B **85** (1991) 327.
[9] K.A. Matveev, Zh. Eksp. Teor. Fiz. **99** (1991) 1598 [Sov. Phys. JETP **72** (1991) 892].
[10] H. Grabert, Phys. Rev. B **50** (1994) 17364.
[11] C.J. Gorter, Physica **17** (1951) 777.
[12] C.A. Neugebauer, and M.B. Webb, J. Appl. Phys. **33** (1962) 74.
[13] I. Giaver and H.R. Zeller, Phys. Rev. Lett. **20** (1968) 1504.
[14] J. Lambe and R.C. Jaklevic, Phys. Rev. Lett. **22** (1969) 1371.
[15] I.O. Kulik, and R.I. Shekter, Zh. Eksp. Teor. Fiz. **68** (1975) 623 [Sov. Phys. JETP **41** (1075) 308].
[16] G.J. Dolan, and J.H. Dunsmuir, Physica B **152** (1988) 7.
[17] T.A. Fulton, and G.J. Dolan, Phys.Rev. Lett. **59** (1987) 109.
[18] K.K. Likharev, and A.B. Zorin, J. Low. Temp. Phys. **59** (1985) 347.
[19] D.V. Averin and K.K. Likharev, J. Low Temp. Phys. **62** (1986) 345.
[20] A. Widom, G. Megaloudis, T.D. Clark, H. Prance and R.J. Prance, J. Phys. A **15** (1982) 3877.
[21] E. Ben-Jacob and Y. Gefen, Phys. Lett. A **108** (1985) 289.
[22] Yu.V. Nazarov, Pis'ma Zh. Eksp. Teor. Fiz. **49** (1989) 105 [JETP Lett. **49** (1990) 126].
[23] M.H. Devoret, D. Esteve, H. Grabert, G.-L. Ingold, H. Pothier and C. Urbina, Phys. Rev. Lett. **64** (1990) 1824.

[24] S.M. Girvin, L.I. Glazman, M. Jonson, D.R. Penn and M.D. Stiles, Phys. Rev. Lett. **64** (1990) 3183.
[25] A.N. Cleland, J.M. Schmidt, and J. Clarke, Phys. Rev. Lett. **64** (1990) 1565.
[26] L.S. Kuzmin, Yu.V. Nazarov, D.B. Haviland, P. Delsing and T. Claeson, Phys. Rev. Lett. **67** (1991) 1161.
[27] K.K. Likharev, IBM J. Res. Dev. **32** (1988) 144.
[28] D.V. Averin and K.K. Likharev, in: Quantum Effects in Small Disordered Systems, B.L. Altshuler, P.A. Lee and R.A. Webb, eds. (Elsevier, Amsterdam, 1991).
[29] G. Schön and A.D. Zaikin, Phys. Rep. **198** (1990) 237.
[30] Single Charge Tunneling, H. Grabert and M.H. Devoret, eds. (Plenum, New York, 1992).
[31] Single Electron Tunneling and Mesoscopic Devices, *Proc. 4th Int. Conf. SQUID* '91, H. Koch and H. Lübbig, eds. (Springer-Verlag, Berlin, 1992).
[32] The Physics of Few-Electron Nanostructures, *Proc. of the Noordwijk NATO ARW*, 1992, L.J. Geerligs, C.J.P.M. Harmans and L.P. Kouwenhoven, eds. (North-Holland, Amsterdam, 1993).
[33] A.N. Cleland, D. Esteve, C. Urbina, and M.H. Devoret, Appl. Phys. Lett. **61** (1992) 2820.
[34] D.A. Fraser, The Physics of Semiconductor Devices (Clarendon, Oxford, 1986).
[35] A. Barone and G. Paterno, Physics and Applications of the Josephson Effect (Wiley, New York, 1982).
[36] See C.W.J. Beenakker, Single Charge Tunneling, H. Grabert and M.H. Devoret, eds. (Plenum, New York, 1992), chap.5 and references therein.
[37] R. Wilkins, E. Ben-Jacob and R.C. Jaklevic, Phys. Rev. Lett. **63** (1989) 801.
[38] C. Schönenberger, H. van Houten and C.W.J. Beenakker, Physica B **189** (1993) 218.
[39] H. Nejoh, Nature **353** (1991) 640.
[40] H. Pothier, P. Lafarge, C. Urbina, D. Esteve, and M.H. Devoret, Physica B **169**, 573 (1991); Europhys. Lett. **17** (1992) 259.
[41] L.J. Geerligs, V.F. Anderegg, P.A.M. Holweg, J.E. Mooij, H. Pothier, D. Esteve, C. Urbina and M.H. Devoret, Phys. Rev. Lett. **64** (1990) 2691.
[42] K. von Klitzing, Rev. Mod. Phys. **58** (1986) 519.
[43] E.R. Williams, R.N. Gosh and J.M. Martinis, J. Res. Natl. Ins. Stand. and Technol. **97** (1992).
[44] D.V. Averin and A.A. Odintsov, Phys. Lett. **A 149**, 251 (1989); D.V. Averin, A.A. Odintsov and S.V. Vyshenskii, J. Appl. Phys. **73** (1993) 1297.
[45] H.D. Jensen and J.M. Martinis, Phys. Rev. B **46** (1992) 13407.
[46] H. Pothier, P. Lafarge, D. Esteve, C. Urbina and M.H. Devoret, IEEE Trans. Instr. and Meas. **42** (1993) 324.
[47] P. Lafarge, P. Joyez, H. Pothier, A. Cleland, T. Holst, D. Esteve, C. Urbina and M.H. Devoret, C. R. Acad. Sci. Paris **314** (1992) 883.
[48] J.M. Martinis, M. Nahum and H. Dalsgaard Jensen, Phys. Rev. Lett. **72** (1994) 904.
[49] T.A. Fulton, P.L. Gammel, D.J. Bishop and L.N. Dunkleberger, Phys. Rev. Lett. **63** (1989) 1307.
[50] L.J. Geerligs, V.F. Anderegg, J. Rommijn and J.E. Mooij, Phys. Rev. Lett. **65** (1990) 377.
[51] L.J. Geerligs, S.M. Verbrugh, P. Hadley, J.E. Mooij, H. Pothier, P. Lafarge, C. Urbina, D. Esteve and M.H. Devoret, Z. Phys. B **85** (1991) 349.
[52] D.V. Averin and Yu.V. Nazarov, Phys. Rev. Lett. **69** (1992) 1993.
[53] M.T. Tuominen, J.M. Hergenrother, T.S. Tighe, and M. Tinkham, Phys. Rev. Lett. **69** (1992) 1997.
[54] P. Lafarge, P. Joyez, D. Esteve, C. Urbina and M.H. Devoret, Phys. Rev. Lett. **70** (1993) 994.
[55] P. Lafarge, Ph. D. thesis, Paris 6 (1993).
[56] T.M. Eiles and J.M. Martinis, Phys. Rev. B **50** (1994) 627.
[57] P. Joyez, P. Lafarge, A. Filipe, D. Esteve and M.H. Devoret, Phys. Rev. Lett. **72** (1994) 2458.
[58] A. Aviram and M. Ratner, Chem. Phys. Lett. **29**, 27 (1974); F.L. Carter, ed., Molecular

Electronic Devices (North-Holland, Amsterdam, 1991).
[59] R.P. Feynman, Optics News (1985) 11.
[60] A.O. Caldeira and A.J. Leggett, Ann. Phys. (N.Y.) **149**(1983) 374; A.J. Leggett in: Chance and Matter, J. Souletie, J. Vannimenus and R. Stora, eds. (North-Holland, Amsterdam, 1987) Course 6.
[61] R. Kubo, Rep. Prog. Phys. **29** (1966) 255.
[62] U. Geigenmüller and G. Schön, Europhys. Lett. **10** (1989) 765.
[63] T. Holst, D. Esteve, C. Urbina and M.H. Devoret, Phys. Rev. Lett. **73** (1994) 3455.
[64] J. Bardeen, L.N. Cooper and J.R. Schrieffer, Phys. Rev. **108** (1957) 1175.
[65] P.W. Anderson, J. Phys. Chem. Solids, **11** (1959) 26.
[66] J.M. Eisenberg and W. Greiner, Nuclear Theory, Vol. 3 (North-Holland, Amsterdam, 1972) Chapter 9.
[67] D. Pines and P. Nozières, Theory of quantum liquids (Benjamin, New York, 1966) Chapter 1.
[68] J. Clarke, in: Non-equilibrium superconductivity, D.N. Langenberg and A.I. Larkin, eds. (North-Holland, Amsterdam, 1986) Chapter 1.
[69] B. Jankó, A. Smith and V. Ambegaokar, Phys. Rev. B **50** (1994) 1152.
[70] M. Tinkham, Introduction to superconductivity [1st ed. by Mc Graw Hill, New York, 1975] (Krieger, Malabar, 1985) Chapter 8.
[71] P. Lafarge, P. Joyez, D. Esteve, C. Urbina and M.H. Devoret, Nature **365** (1993) 422.